DISSERTATION

TROPICAL TEVELEV DEGREES

Submitted by

Erin Dawson

Department of Mathematics

In partial fulfillment of the requirements

For the Degree of Doctor of Philosophy

Colorado State University

Fort Collins, Colorado

Spring 2025

Doctoral Committee:

Advisor: Renzo Cavalieri

Maria Gillespie
Rick Miranda
Silvia Canetto

ABSTRACT

TROPICAL TEVELEV DEGREES

Tropical Hurwitz spaces parameterize genus g, degree d covers of a tropical rational curve with fixed branch profiles. Since tropical curves are metric graphs, this gives us a combinatorial way to study Hurwitz spaces. Tevelev degrees are the degrees of a natural finite map from the Hurwitz space to a product $\overline{\mathscr{M}}_{g,n} \times \overline{\mathscr{M}}_{0,n}$. In 2021, Cela, Pandharipande and Schmitt presented this interpretation of Tevelev degrees in terms of moduli spaces of Hurwitz covers. We define the *tropical Tevelev degrees*, $\mathsf{Tev}_g^{\mathtt{trop}}$ in analogy to the algebraic case. We develop an explicit combinatorial construction that computes $\mathsf{Tev}_g^{\mathtt{trop}} = 2^g$. We prove that these tropical enumerative invariants agree with their algebraic counterparts, giving an independent tropical computation of the algebraic degrees Tev_g. We finally generalize tropical Tevelev degrees to more cases and construct computations of these invariants.

ACKNOWLEDGEMENTS

First, I would like to thank my advisor, Renzo Cavalieri, for all of his guidance over the last few years. Thank you for encouraging me when I needed it and supporting various travels during my time here at CSU that helped shape me as a mathematician.

I am grateful for my family for their endless support and love. Thanks for always encouraging me to follow my dreams and do what makes me happy. I wouldn't have been able to do this without them.

Thank you to my friends near and far, for being there for me for the past 5 years. They made this experience fun. I will cherish the memories of game nights, brewery visits, bonfires, hiking adventures, boating, and more.

To Davis, thank you for being my rock. I couldn't have made it through graduate school without you by my side.

TABLE OF CONTENTS

LIST OF FIGURES

Chapter 1

Introduction

One commonly studied branch of algebraic geometry is enumerative geometry. Enumerative geometry seeks to answer questions of the form: how many geometric objects satisfy given conditions? These types of questions can be translated into the study of the geometry of moduli spaces. For example, the question how many lines go through 2 points in the plane is the same as studying the moduli space of lines in $\mathbb{P}^2$. This dissertation specifically involves computing the degree of a map between two tropical moduli spaces. This is an example of a combinatorial inverse problem because we are counting graphs that map to the same image via a specific finite map. A key aspect of this work is the study of Tevelev degrees, with the goal of this dissertation being to tropicalize Tevelev degrees of $\mathbb{P}^1$.

Tevelev degree is an enumerative invariant that counts the number of curves satisfying certain conditions. More precisely, studying Tevelev degrees involves exploring the following question:

Question: Let X be a smooth, projective variety, let C be a curve of genus g containing points $p_1,\dots,p_n$, let $\beta \in H_2(X,\mathbb{Z})$ be a curve class on X, and let $q_1,\dots,q_n \in X$ be general points. Then, how many morphisms $f : C \to X$ are there such that $f_*([C]) = \beta$ and satisfying $f(p_i) = q_i$ for $i = 1,2,\dots,n$?

Equivalently, this question is asking for the degree of the following morphism

$$\tau : \mathscr{M}_{g,n}(X,\beta) \to \mathscr{M}_{g,n} \times X^n.$$

Assuming the expected dimension of $\mathscr{M}_{g,n}(X,\beta)$ is equal to the dimension of $\mathscr{M}_{g,n} \times X^n$, the answer is referred to as a *geometric Tevelev degree* of X. The name comes from Tevelev studying the case $X = \mathbb{P}^1$ and $n = g+3$ in [1]. Tevelev was motivated by physics and referred to the count as the degree of the *scattering amplitude map*. One can alternatively formulate a virtual analogue of the question in Gromov-Witten theory. These counts are referred to as *virtual Tevelev degrees*

and are explored in [2]. Via the Gromov-Witten theoretic approach, Tevelev degrees to higher dimensional targets have been studied in [3–5]. Specifically when X is a Hirzebruch surface, this question has been investigated using tropical geometry in [5].

Tevelev degrees appeared in the literature prior to this. In 1991, Kenneth Intriligator introduced the physical Vafa-Intriligator formula, which is a result in quantum field theory and string theory [6]. A special case of this formula predicts the number of maps from a curve C to a Grassmannian satisfying incidence conditions with Schubert cycles which was studied by Bertram [7]. This enumerative problem was imported into mathematics and translated to a question of virtual intersection theory on the Quot scheme; various approaches and proofs of the formula have appeared in [8–10].

Focusing on the case $X = \mathbb{P}^1$, Tevelev degrees can be reformulated from the point of view of the moduli space of Hurwitz covers as done in [11]. The authors interpret the family of scattering amplitude maps parameterized by genus g curves as the product $f_s \times f_t$ of source and target forgetful morphisms from a Hurwitz space, see Section 2.3 for details. For any integer ℓ, if we set $d = g+1+\ell$ and $n = g+3+2\ell$, the maps $f_s \times f_t$ remain finite. The problem becomes looking at the degree of the following morphism:

$$f_s \times f_t : \overline{\mathscr{H}}_{g,d,n} \to \overline{\mathscr{M}}_{g,n} \times \overline{\mathscr{M}}_{0,n}.$$

In [11], the authors solve for Tevelev degrees by using excess intersection theory to come up with a recursion. To generalize these results, one can require non-generic ramification orders in the space of admissible covers, this case has been studied in [12].

This set up when $X = \mathbb{P}^1$ is the jumping off point of this dissertation. This work aims to tropicalize Tevelev degrees of $\mathbb{P}^1$.

One of the common mantras of tropical techniques in enumerative geometry is that tropical geometry is a powerful tool to organize the combinatorics of the degeneration formula for curves. In light of our better understanding of the relationship beteween algebraic and tropical geometry brought about by their fitting together into the picture of logarithmic geometry, we can now say that the tropical perspective goes well beyond a mere organization of algebraic geometric information. To illustrate this point, let us observe the morphism $f_s \times f_t : \overline{\mathscr{H}}_{g,d,n} \to \overline{\mathscr{M}}_{g,n} \times \overline{\mathscr{M}}_{0,n}$ whose

degree gives the Tevelev degree Tev_g. While the inverse image of a generic point in the interior of $\overline{\mathscr{M}}_{g,n} \times \overline{\mathscr{M}}_{0,n}$ consists of the correct number of points, we have no algebraic geometric technique to even *name* general smooth curves, let alone reconstruct covers with specified source and target. The degeneration formula approach is based on the fact that both source and target of $f_s \times f_t$ are stratified spaces, which hands us privileged choices for points: the zero dimensional strata, parameterizing the most degenerate curves. In an ideal world, the inverse image of a zero dimensional stratum would consist of a collection of zero dimensional strata, perhaps lots of them, perhaps to be counted with some multiplicities - and tropical geometry would serve as a book-keeping device for this combinatorics. In reality, in spaces of admissible covers nodes of source curves and their images do not smooth independently, which as a consequence causes the inverse images of zero dimensional strata to be positive dimensional. In addition to solving a combinatorial problem, one has to then also correct for excess intersection. This is the approach of [11]: however, to avoid having to deal with the amount of excess intersection coming from zero dimensional strata, they limit themselves to pulling back low codimension strata and then obtain recursions among auxiliary types of Tevelev degrees; thus they need to enlarge their scope in order eventually solve the recursions for the original invariants.

Tropical geometry witnesses this failure of transversality as follows: the tropicalized map $F_s \times F_t$ is not a strict map of cone complexes, as smaller dimensional cones are mapped to the relative interior of larger dimensional cones. This also suggest a remedy for the situation: appropriate refinements of the cone complex structures of target and source can make $F_s \times F_t$ a strict map; this corresponds to appropriate birational modifications of the algebraic spaces in such a way that the morphism $f_s \times f_t$ extends to a map with zero dimensional fibers. There are new zero dimensional strata, parameterizing curves and covers with logarithmic structures, and the count of their inverse image is now completely combinatorial (with no excess intersection); this is in essence the idea driving the correspondence theorem. A more extensive introduction to this circle of ideas may be found in D. Ranganathan lecture notes collected in [13].

A further advantage of the tropical approach is that the identification of the inverse images and their multiplicities may be done entirely in the realm of combinatorics: the tropical information of the logarithmic curves and covers is sufficient for this computation. At this point, the challenge is to choose a maximal dimensional cone of the refinement of the cone complex $\mathscr{M}_{g,n}^{\mathtt{trop}} \times \mathscr{M}_{0,n}^{\mathtt{trop}}$ corresponding to tropical curves for which it is possible to solve the combinatorial inverse problem.

The reason that this is more complicated than one initially expects is that for tropical admissible covers, lengths of edges of source and cover curves are not independent. But since for a top dimensional cone in $\mathscr{M}_{g,n}^{\mathtt{trop}} \times \mathscr{M}_{0,n}^{\mathtt{trop}}$ all lengths should be deformable independently, we must be looking for somewhat exotic tropical admissible covers where no edge of the stabilization of the source curve maps to one or a collection of edges of the stabilization of the target curve.

The strategy we settled on eventually consists in separating genus part of the cover from the marked ends: $\overline{\Gamma}$ contains an umnmarked chain of loops with independent edges, to which is attached a tree with all the marked points. The lengths of the stabilized target $\overline{T}$ are chosen uncomparably longer than the edges of $\overline{\Gamma}$. These choices cause two structural advantages in searching for covers $\phi : \Gamma \to T$ stabilizing to $(\overline{\Gamma}, \overline{T})$:

1. the chain of loop structure, together with a Riemann-Hurwitz count shows that the loops of the cover must be formed with a very small number of transpositions, and two points of very high ramification order: this restricts considerably the number of options of how loops are formed and allows for classification.

2. the marked ends being all part of one tree forces their inverse images to lie on different copies of a small number of fragments of the same tree, and this structure allows for classification.

In conclusion, the careful choice of the point $p = (\overline{\Gamma}, \overline{T})$ in a maximal cone of the refinement of $\mathscr{M}_{g,n}^{\mathtt{trop}} \times \mathscr{M}_{0,n}^{\mathtt{trop}}$ allows for a concrete combinatorial reconstruction of the inverse images. After having proven the correspondence theorem, these computations of Tevelev degrees are certainly more direct and less sophisticated than the previous proofs in the literature. We hope that this type of approach might extend our reach to similar enumerative geometric problems involving counts of curves related to intersection problems on moduli spaces with high amounts of excess intersection.

This dissertation is organized as follows. In Chapter 2, we give the necessary background information and introduce notation. In Chapter 3, we define tropical Tevelev degrees, prove the correspondence theorem and compute the first case of tropical Tevelev degrees of $\mathbb{P}^1$ as presented in [14]. For an integer ℓ, we can generalize the conditions on degree and the number of marked points to let $d = g + 1 + \ell$ and $n = g + 3 + 2\ell$. In Chapter 4, we generalize tropical Tevelev degrees to positive and negative values of ℓ and provide computations of each case.

Chapter 2

Background

2.1 Tropical curves

In this section we recall necessary definitions of tropical curves and their moduli spaces from [15]. A *tropical curve* with genus g and n marked points is a metric graph Γ with a genus function $g : \Gamma \to \mathbb{N}$ such that:

- the marked points are the unbounded ends;
- the genus is given by

$$g(\Gamma) = h_1(\Gamma) + \sum_{p \in \Gamma} g(p).$$

The *combinatorial type* is the equivalence class of curves that differ only by the lengths of their bounded edges. A tropical curve is said to be *stable* if every genus 0 vertex has valence 3 or more.

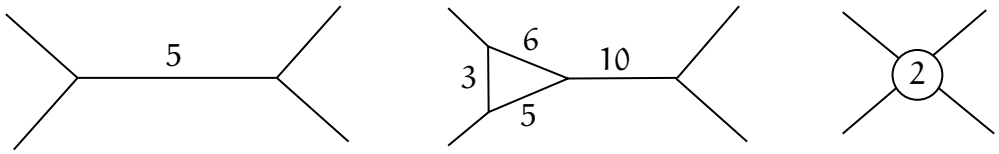

Figure 2.1: Three examples of stable tropical curves all with 4 marked points. The genus of each from left to right is $0, 1$ and 2. The example on the right demonstrates a genus of a vertex that is not zero.

The set of all tropical curves of a fixed combinatorial type can be parameterized by all positive lengths for each bounded edge, this gives a positive orthant. If the underlying graph has automorphisms, then we must identify points of the orthant accordingly. The *dimension* of a combinatorial type is the number of bounded edges, this dimension is equal to the dimension of the corresponding orthants. These orthants are *cones*, and can be glued together to form an *abstract cone complex* as demonstrated in Figure 2.2. Formally, the moduli space $\mathscr{M}_{g,n}^{\mathrm{trop}}$ is the abstract cone complex

parameterizing all stable tropical curves of genus g with n marked points that is the obtained as the topological colimit

$$\mathscr{M}_{g,n}^{\mathtt{trop}} = \varinjlim\{\sigma_\Theta\}$$

where Θ ranges over the combinatorial types, the face morphisms are given by automorphisms of tropical covers and edge contractions.

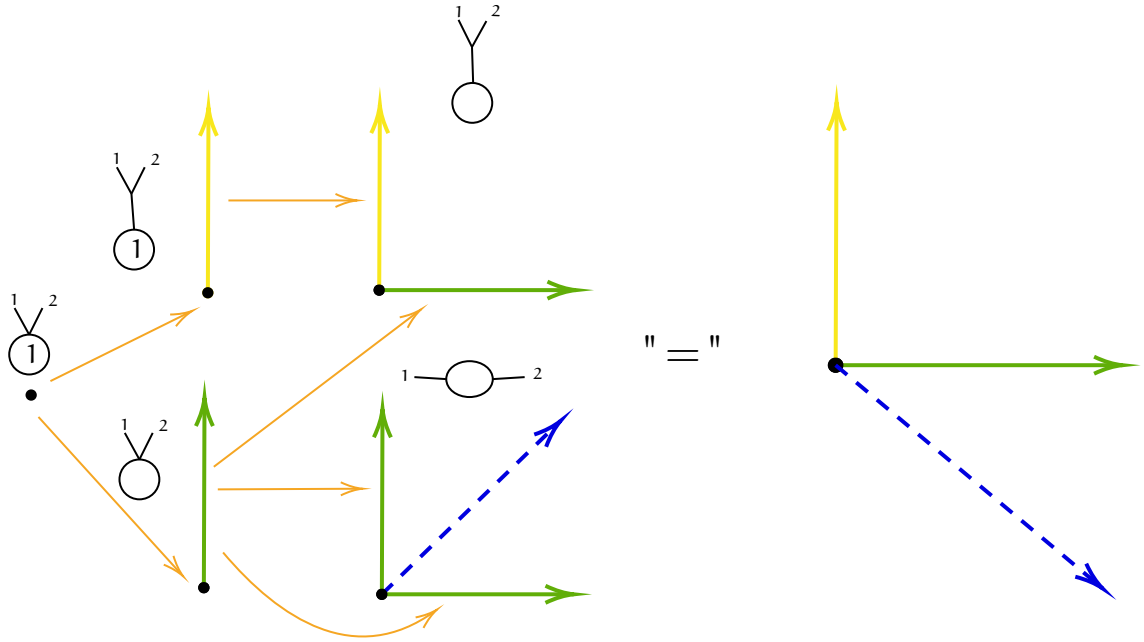

Figure 2.2: The left hand side shows all combinatorial types in $\mathscr{M}_{1,2}^{\mathtt{trop}}$ with their corresponding cone. Note that the combinatorial type on the bottom right has an automorphism of switching the 1 and the 2, the corresponding cone is folded, which is represented by the blue dashed line. The orange arrows show how the cones are glued together when an edge can be added to get from one combinatorial type to the next. Taking the colimit of the left hand side gives the right hand side, which shows the abstract cone complex for $\mathscr{M}_{1,2}^{\mathtt{trop}}$ obtained when the cones are glued together.

2.2 Hurwitz numbers

Let X and Y be Riemann Surfaces and $f : X \to Y$ be a non-constant, degree d, holomorphic map. We recall the following definitions from [16].

- Given a point $x \in X$, the integer k_x, such that there exists a local expression centered at p of the form $F(z) = z^{k_x}$, is called the *ramification index* of f at x.
- If a point x has ramification index $k_x = 1$, then we say f is *unramified* at x.
- A point x such that $k_x \geq 2$ is called a *ramification point* and $f(x) \in Y$ is called a *branch point*.
- Let $y \in Y$ and $f^{-1}(y) = \{x_1, \ldots, x_n\}$. We call the set $\{k_{x_1}, \ldots, k_{x_n}\}$ the *ramification profile* of f at y. Note that the ramification profile is a partition of d.
- If the ramification profile of f at y is:
  - $(1, \ldots, 1)$, then f is *unramified* over y;
  - (2) or $(2, 1, \ldots, 1)$, then f has *simple ramification* over y.

When X and Y are compact Riemann Surfaces, the following formula gives a relation among the invariants.

Theorem 2.2.1 (Riemann-Hurwitz Formula)**.** *Let* $f : X \to Y$ *be a non-constant, degree* d *holomorphic map. Denote by* g_X *(respectively* g_Y*) the genus of* X *(respectively* Y*). Then*

$$2g_X - 2 = d(2g_Y - 2) + \sum_{x \in X} (k_x - 1). \tag{2.1}$$

We call f a *Hurwitz cover* when the following are satisfied:

- f is a holomorphic map;
- X is connected, compact, and has genus g;
- $\{b_1, \ldots, b_n\}$ are the branch points;
- the ramification profile of f at b_i is λ_i.

Hurwitz covers are only possible when the Riemann-Hurwitz formula is satisfied. The *Hurwitz number* is the weighted sum over each isomorphism class of Hurwitz covers. More formally, the Hurwitz number is

$$H_{h\to g,d}(\lambda_1,\ldots,\lambda_n) = \sum_{[f]} \frac{1}{|\mathrm{Aut}(f)|}$$

where f is a Hurwitz cover [16].

Hurwitz numbers are frequently studied when Y is the projective line. In this case they are counting the number of covers of the projective line. In 2008, Cavalieri, Johnson and Markwig tropicalized Hurwitz numbers of the projective line [17]. They define the *tropical Hurwitz number* as the degree of the branch morphism

$$\begin{aligned} \mathrm{br} : \mathscr{M}_g^{\mathrm{trop}}(\mathbb{P}^1,\Delta) &\to \mathbb{R}^{\#\Delta-2+2g} \\ (\Gamma,f) &\to (f(V_1),\ldots,f(V_{\#\Delta-2+2g})) \end{aligned}$$

where V_i is the vertex or point with label i. They also prove that there is a correspondence between the tropical Hurwitz number and the algebraic Hurwitz number.

2.3 Algebraic Tevelev degrees

We assume familiarity with the moduli spaces of curves and their Deligne-Mumford compactifications, see [18, 19] for introductory presentations.

By $\overline{\mathscr{H}}_{g,d,n}$ we denote the admissible cover compactification ([20]) of the Hurwitz space whose points parameterize isomorphism classes of covers $\varphi : C \to \mathbb{P}^1$ such that:

- C is a connected smooth curve of genus g;
- φ is a map of degree d;
- all ramification points of φ are simple and marked;
- n unramified points of C are marked.

The space of admissible covers admits natural source and branch morphisms:

$$\begin{aligned} \mathrm{src} &: \overline{\mathscr{H}}_{g,d,n} \to \overline{\mathscr{M}}_{g,2g+2d-2+n} \\ \mathrm{br} &: \overline{\mathscr{H}}_{g,d,n} \to \overline{\mathscr{M}}_{0,2g+2d-2+n} \end{aligned} \tag{2.2}$$

Define $f_s := \pi_R \circ \mathrm{src}$ by postcomposing the source morphism with the forgetful morphism forgetting the $2g+2d-2$ marks corresponding to ramification points; similarly, $f_t := \pi_B \circ \mathrm{br}$ is obtained composing the branch morphism with the morphism forgetting the marks corresponding to branch points. Consider the map

$$f_s \times f_t : \overline{\mathscr{H}}_{g,d,n} \to \overline{\mathscr{M}}_{g,n} \times \overline{\mathscr{M}}_{0,n}. \tag{2.3}$$

When $d = g+1$ and $n = g+3$, $f_s \times f_t$ is a finite morphism of $5g$-dimensional spaces. We observe that in this case the cardinality of the ramification (or equivalently branch) locus of any cover $\varphi : C \to \mathbb{P}^1$ is $4g$. In [11, Section 1.2] the *Tevelev degree* is defined as:

$$\mathsf{Tev}_g := \frac{\deg(f_s \times f_t)}{(4g)!}. \tag{2.4}$$

In [1], an equivalent definition is given for Tevelev degrees (called in that paper degrees of the scattering amplitude map), and in Theorem 1.13 it is proved that $\mathsf{Tev}_g = 2^g$.

2.4 Tropical admissible covers

We assume familiarity with moduli spaces of tropical curves ([15, 21]) and the tropicalization statement from [22], that identifies the cone complex $\mathscr{M}_{g,n}^{\mathtt{trop}}$ with the Berkovich skeleton of the analytification of $\mathscr{M}_{g,n}$ as a dense open set inside its Deligne-Mumford compactification $\overline{\mathscr{M}}_{g,n}$. Unless otherwise specified, we assume all ends of a tropical curve to be labeled.

Tropical admissible covers were introduced in [23]; their moduli spaces and a tropicalization statement were studied in [24]. We recall some of the statements that are useful in the remainder of the paper.

A *tropical admissible cover* of a rational tropical curve with labeled ends is a morphism of tropical curves $\phi : \Gamma \to T$ satisfying the following requirements:

1. T is a stable tree with labeled ends.

2. Parameterizing the relevant edges by arc length (with $\phi(0_e) = 0_{\phi(e)}$), the restriction of ϕ to an edge e is a linear function
$$\phi|_e : [0, l_e] \to [0, l_{\phi(e)}], \tag{2.5}$$
where l_x denotes the length of the edge x. The slope $m_e = l_{\phi(e)}/l_e$ is required to be a positive integer, and it is also called the *expansion factor* or the *degree* of the edge e.

3. The map ϕ is *harmonic*, i.e. for any vertex $v \in \Gamma$ and pairs of edges $e_1, e_2 \in T$ incident to $\phi(v)$, we have:
$$\sum_{\substack{e \ni v \\ \phi(e) = e_1}} m_e = \sum_{\substack{e \ni v \\ \phi(e) = e_2}} m_e \tag{2.6}$$
The quantity in (2.6) is a well-defined invariant of the vertex v, called the *local degree* of ϕ at v. By harmonicity we have a well-defined notion of *degree* of ϕ, which may be defined equivalently as either the sum of the local degrees of all vertices in the inverse image of a given vertex of T, or the sum of the expansion factors of all edges in the inverse image of a given edge of T.

4. The *local Riemann-Hurwitz condition* is satisfied at every vertex v of Γ, i.e.
$$\mathrm{val}_v + 2g_v - 2 = d_v(\mathrm{val}_{\phi(v)} - 2); \tag{2.7}$$
here val stands for valence, g_v is the genus of the vertex v and d_v is the local degree of ϕ at v.

The *combinatorial type* Θ of a tropical admissible cover $\phi : \Gamma \to T$ is the data obtained forgetting all metric information for Γ and T, but remembering expansion factors of edges of Γ.

The set of admissible covers of a given combinatorial type Θ is naturally parameterized by the cone $\sigma_\Theta = \mathbb{R}_{\geq 0}^{|CE(T)|}$, where $CE(T)$ denotes the set of compact edges of T. For e any compact edge of T, let $M_e := \mathrm{lcm}(\{m_{e'} | e' \in \Gamma, \phi(e') = e\})$. We define an integral structure in σ_Θ by requiring the lengths of all compact edges of Γ and T to be integers. We obtain:

$$\Lambda_\Theta := \mathbb{R}_{\geq 0}^{|CE(T)|} \cap \bigoplus_{e \in CE(T)} M_e \cdot \mathbb{Z}. \tag{2.8}$$

We now define the discrete data that identifies a moduli space of tropical admissible covers. We call *Hurwitz data* the tuple $\mathfrak{h} = (g, d, N, \lambda_1, \ldots, \lambda_N)$, where g, d, N are non-negative integers and the λ_i's are partitions of the integer d. A combinatorial type Θ of tropical admissible covers satisfies the Hurwitz data $\mathfrak{h}$ if the genus of Γ is equal to g, T has N labeled ends, the degree of ϕ is d and the collection of expansion factors for the ends of Γ above the i-th marked end of T agrees with the partition λ_i. We refer to λ_i as the *branching data* for the i-th end of T.

There are finitely many combinatorial types Θ satisfying a given Hurwitz data $\mathfrak{h}$, we denote this finite set by $\Theta_\mathfrak{h}$. The moduli space of *tropical admissible covers of type* $\mathfrak{h}$ is the (generalized) cone complex obtained as the colimit

$$\mathscr{H}_\mathfrak{h}^{\mathtt{trop}} = \varinjlim \{\sigma_\Theta\}_{\Theta \in \Theta_\mathfrak{h}}, \tag{2.9}$$

where the face morphisms are given by automorphisms of tropical covers and edge contractions as described in [24, Section 3.2.5].

It is convenient to give the moduli space $\mathscr{H}_\mathfrak{h}^{\mathtt{trop}}$ the structure of a weighted cone complex, by giving maximal dimensional cones σ_Θ the weight

$$w(\Theta) := \frac{1}{|\mathrm{Aut}(\Theta)|} \cdot \prod_{v \in V(\Gamma)} H_v \cdot \prod_{e \in CE(T)} \frac{\prod_{\phi(e')=e} m_{e'}}{M_e}, \tag{2.10}$$

where H_v denotes the *local Hurwitz number* associated to the vertex v ([24, Section 3.2.4]).

2.5 Tropical intersection theory

Since its early days, tropical geometry has been applied as a powerful tool for transforming classical problems in enumerative geometry into a combinatorial framework. Recasting these complex geometric problems in a more combinatorial setting allows for novel insights and methods of computation.

To achieve this goal, Mikhalkin [25] laid down the foundational principles of tropical intersection theory. In his work, he introduced the concepts of tropical cycles and defined their stable intersections, which provided an intial framework for understanding how intersection products could be handled in a tropical setting. His contributions opened the door for a combinatorial interpretation of classical intersection theory. Building on this foundation, Allerman and Rau [26] presented an alternative approach to defining intersection products. Their method involved the pull-back of Cartier divisors. This alternative formulation enriched the theory by providing additional tools and viewpoints for approaching intersection problems within tropical geometry. Further solidifying these developments, Katz [27] demonstrated the equivalence of these two different constructions by connecting both to toric intersection theory.

The development of tropical intersection theory did not stop with these initial constructions. Shaw [28] extended the concept by generalizing the intersection product to locally matroidal fans. This generalization broadened the scope of tropical intersection theory, allowing it to be applied in the context of matroid theory. Tropical intersection theory was further broadened when Gross [29] extending these ideas to weakly embedded cone complexes. These complexes arise from the tropicalizations of cycles on toroidal embeddings.

2.6 Tropical fans

In this section we recall some definitions and ideas of tropical intersection theory from [30]. Let Λ denote a finitely generated free abelian group and $V := \Lambda \otimes_{\mathbb{Z}} \mathbb{R}$ the corresponding real vector space. Λ is considered a lattice in V. The dual lattice is denoted $\Lambda^\vee$.

A *cone* is a subset $\sigma \subset V$ given by finitely many linear integral equalities and inequalities,

$$\sigma = \{x \in V | f_i(x) = 0 \text{ for all } i = 1, \ldots, n \text{ and } g_j(x) \geq 0 \text{ for all } j = 1, \ldots, m\}$$

for some $f_1, \ldots, f_n, g_1, \ldots, g_m \in \Lambda^\vee$. A *fan* X in V is a finite set of cones in V such that

- all faces of the cones in X are also in X;
- the intersection of any two cones in X is a face of each.

The union of all cones in X is denoted $|X|$.

The smallest vector subspace of V that contains σ is denoted V_σ. The *dimension* of σ is $\dim\sigma := \dim V_\sigma$. The biggest dimension of a cone in a fan X is the *dimension* of X. A fan is *pure-dimensional* if each maximal cone in X has this dimension.

A *weighted fan* is a pair (X, ω_X) where X is a pure-dimensional fan of dimension n in V, and ω_X is a map from the set of all n-dimensional cones of X to $\mathbb{Z}_{>0}$. The weight of a cone is $\omega_X(\sigma)$. A *tropical fan* is a weighted fan such that for all cones τ of dimension one less than the dimension of X, the balancing condition

$$\sum_{\sigma > \tau} \omega_X(\sigma) \cdot u_{\sigma/\tau}$$

holds, where $u_{\sigma/\tau}$ denotes the primitive normal vector.

A fan Y is called a *subfan* of X ($Y \subset X$) if each cone of Y is contained in a cone of X. We denote by $C_{Y,X} : Y \to X$ the map that sends a cone σ in Y to the cone in X that contains σ. Let (X, ω_X) and (Y, ω_Y) be weighted fans in V. (Y, ω_Y) is a *refinement* of (X, ω_X) if

- $Y \subset X$

- $|Y|=|X|$
- $\omega_Y(\sigma) = \omega_X(C_{Y,X}(\sigma))$ for all maximal cones in Y

Let X be a fan in $V = \Lambda \otimes \mathbb{R}$, and let Y be a fan in $V' = \Lambda' \otimes \mathbb{R}$. A *morphism of fans* $f : X \to Y$ is a map from $|X|$ to $|Y|$ such that f is induced by a linear map from Λ to Λ'. A morphism of weighted fans is a morphism of fans.

2.7 Degrees of tropical morphisms

In this section we recall some standard facts about the notions of degree of maps of tropical objects. We use tropical intersection theory ideas to compute degrees by counting the inverse images, with multiplicities, of a point in a maximal cone. For a more comprehensive introduction to tropical intersection theory see, for example, [31, Section 6.7].

Let Σ_1, Σ_2 be two generalized, weighted cone complexes obtained as colimits of collections of smooth cones with integral structures (i.e. they are simplicial and the primitive vectors along the rays generate the integral structure). We assume for simplicity of exposition that there are no self-maps (automorphisms of the cone preserving the integral structure) in the systems: else, one includes a factor of $1/|\mathrm{Aut}(\sigma)|$ in the weight $w(\sigma)$ of each top dimensional cone σ and what follows goes through otherwise unchanged.

Assume Σ_1, Σ_2 are pure dimensional of equal dimension m, and let $F : \Sigma_1 \to \Sigma_2$ be a strict morphism of generalized cone complexes; in particular, for any maximal cone $\sigma \in \Sigma_1$, its image is a cone $\sigma' \in \Sigma_2$; the restriction $F|_\sigma : \sigma \to \sigma'$ is a linear function that preserves the integral structures in the sense that $F(\Lambda_\sigma) \subseteq \Lambda_{\sigma'}$.

With all this notation in place, we make the following definitions.

Definition 2.7.1. For a morphism $F : \Sigma_1 \to \Sigma_2$ as introduced in the previous paragraphs, we have the following notions of degree:

local degree at a point in the source let $x \in \Sigma_1$ be a point in the relative interior of a maximal cone $\sigma \in \Sigma_1$. We define the local degree at x to be

$$\deg_x F := \begin{cases} 0 & \text{if } \dim F(\sigma) < \dim \sigma, \\ \frac{w(\sigma)}{w(F(\sigma))}[\Lambda_{F(\sigma)} : F(\Lambda_\sigma)] & \text{if } \dim F(\sigma) = \dim \sigma \end{cases} \tag{2.11}$$

local degree above a point in the target let $y \in \Sigma_2$ be a point in the relative interior of a maximal cone $\sigma' \in \Sigma_2$. We define the local degree above y to be

$$\deg_y F := \sum_{x \in F^{-1}(y)} \deg_x F. \tag{2.12}$$

global degree if the local degree above a point in the target is independent of the choice of the point, it gives a well-defined notion of global *degree*, i.e.

$$\deg F := \deg_y F, \quad \text{if for any } y', \deg_{y'} F = \deg_y F. \tag{2.13}$$

There are combinatorial criteria that imply that the degree of a morphism of cone complexes is well-defined. The most explored situation is the case in which Σ_1 and Σ_2 are fans, i.e. they are embedded in vector spaces from which they inherit their integral structures. Another technique is to show that F arises as the tropicalization of an algebraic map with a well-defined degree.

We conclude this section with an elementary statement about how to compute the lattice index in (2.11). Let M_σ be the $m \times m$ matrix representing the linear function $F|_\sigma$ in the bases given by the primitive integral generators of the rays of σ and $F(\sigma)$; then

$$[\Lambda_{F(\sigma)} : F(\Lambda_\sigma)] = |\det(M_\sigma)|. \tag{2.14}$$

Chapter 3

Tropical Tevelev Degrees

This work has two main, synergistic objectives: the first is to introduce a family of tropical enumerative geometric invariants inspired by, and agreeing with a corresponding family of algebraic enumerative invariants. The second is to perform an explicit combinatorial computation of these invariants.

For any non-negative integer g, let $d = g+1$ and $n = g+3$. These conditions are chosen so that the dimension of the moduli space of tropical admissible covers $\mathscr{H}^{\mathtt{trop}}_{g,d,n}$ (see Definition 3.1.1 for details) equals the sum of the dimensions of $\mathscr{M}^{\mathtt{trop}}_{g,n}$ and $\mathscr{M}^{\mathtt{trop}}_{0,n}$. The product of forgetful morphisms $\mathsf{F}_s \times \mathsf{F}_t$, forgetting the cover map but remembering the source and target as n-pointed curves is then a finite map, and the *tropical Tevelev degree* $\mathsf{Tev}^{\mathtt{trop}}_g$ is defined to be its degree. There is an algebraic version of Tevelev degrees which is defined analogously and denoted Tev_g. Our first main result is a correspondence theorem.

Theorem 3.0.1. *For any g, we have*

$$\mathsf{Tev}^{\mathtt{trop}}_g = \mathsf{Tev}_g. \tag{3.1}$$

Computing tropical Tevelev degrees is a combinatorial inverse problem: given a pair $(\overline{\Gamma}, \overline{T})$ of general n-marked tropical curves of genera g and 0, one must find all possible tropical covers $\phi : \Gamma \to T$ whose source stabilizes to $\overline{\Gamma}$ and target stabilizes to $\overline{T}$ when all ends are forgotten except the n marks. While this can be a very complicated task, we choose a pair $(\overline{\Gamma}, \overline{T})$[1] that allows for a richly combinatorial reconstruction of these inverse images, as well as for the computation of their multiplicities. We obtain our second main result.

[1] while the notion of a point in "special-general" position seems self-contradictory, it is a commonly used notion in enumerative geometry; in this particular case, what we mean is that the point can be choosen in the relative interior of a maximal dimensional cone in some cone complex which appropriately refines $\mathscr{M}^{\mathtt{trop}}_{g,n} \times \mathscr{M}^{\mathtt{trop}}_{0,n}$.

Theorem 3.0.2. *For any positive integer* g*,*

$$\mathsf{Tev}_g^{\mathtt{trop}} = 2^g.$$

The following immediate corollary shows that this is an instance in which tropical geometry can provide an independent proof for an algebraic statement.

Corollary 3.0.3. *Theorem 3.0.2 and Theorem 3.0.1 together provide a tropical proof of [1, Theorem 1.13], showing* $\mathsf{Tev}_g = 2^g$.

3.1 Tropical Tevelev degrees and correspondence

We make a definition of tropical Tevelev degrees following the algebraic one from [11]. We will consider the tropical version of the morphism from (2.3): it is a map of weighted cone complexes with integral structures, for which we have defined a notion of local degree above any general point of the target in Definition 2.7.1. The correspondence theorem (Theorem 3.0.1) implies that this notion gives a well defined global degree, since that's the case on the algebraic side.

For any non-negative integer g, consider the Hurwitz data

$$\mathfrak{h}(g) = (g, d = g+1, N = 5g+3, \eta_1, \ldots, \eta_{5g+3}), \tag{3.2}$$

where

$$\eta_i = \begin{cases} (1,\ldots,1) & i \leq g+3 \\ (2,1,\ldots,1) & g+4 \leq i \leq 5g+3 \end{cases} \tag{3.3}$$

Definition 3.1.1. For any non-negative integer g let $n = g+3$ and define by $\mathscr{H}^{\mathtt{trop}}_{g,d,n}$ to be the variant of the moduli space of tropical admissible covers $\mathscr{H}^{\mathtt{trop}}_{\mathfrak{h}(g)}$ where:

- $\mathfrak{h}$ is the Hurwitz data from (3.2);
- for $i \leq g+3$, only one end of Γ in the inverse image of the i-th end of T is marked;
- for $i > g+3$, the marked ends of T and of their inverse images in Γ are not marked.

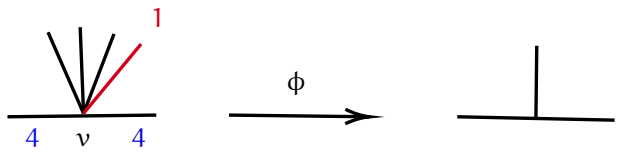

Figure 3.1: A local fragment of a tropical cover $\phi : \Gamma \to \mathsf{T}$ near a vertex v of local degree 4. The blue 4's denote the expansion factors of the edges, which are assumed to be compact edges of Γ. Diagonally, we have ends of Γ, only one of which is marked (depicted in red). The local Hurwitz number for v is equal to 1: the triple Hurwitz number $H_0((4),(4),(1,1,1,1))$ with all ends marked is equal to 6, but we divide by a factor of 6 corresponding to permuting the black ends. Such a factor is incorporated in the local Hurwitz number and is no longer counted as part of the automorphisms of the cover.

We are violating here the convention we stated earlier about all ends of tropical curves being labeled; the spaces thus obtained are finite (cone stack) quotients of the tropical admissible cover spaces defined in Section 2.4; in practice this will cost us having to pay attention to some additional automorphisms, but this choice both simplifies the combinatorics we will encounter and makes the definition of tropical Tevelev degrees more natural. In particular, we make the following convention about local Hurwitz numbers.

Convention 3.1.2. Consider an admissible cover $\phi : \Gamma \to \mathsf{T}$, and suppose a vertex $v \in \Gamma$ is adjacent to a certain number n of unmarked ends mapping to the same end of T. Then the automorphism factor $1/n!$ consisting of permuting these ends is incorporated in the local Hurwitz number, rather than in the automorphism factors. See Figure 3.1 for an illustration.

There are natural source and branch morphisms:

$$\begin{aligned} \mathrm{src}^{\mathtt{trop}} &: \mathscr{H}^{\mathtt{trop}}_{g,d,n} \to \mathscr{M}^{\mathtt{trop}}_{g,5g+3} \\ \mathrm{br}^{\mathtt{trop}} &: \mathscr{H}^{\mathtt{trop}}_{g,d,n} \to \mathscr{M}^{\mathtt{trop}}_{0,5g+3} \end{aligned} \tag{3.4}$$

Analogously to the construction in Section 2.3, we postcompose these morphisms with the forgetful morphisms that forget the last $4g$ ends of T and the corresponding marked ends of Γ in

their inverse image, and obtain forgetful morphisms:

$$\begin{aligned} F_s &= \pi_{\{i \geq g+4\}} \circ \mathrm{src}^{\mathtt{trop}} \\ F_t &= \pi_{\{i \geq g+4\}} \circ \mathrm{br}^{\mathtt{trop}}. \end{aligned} \tag{3.5}$$

Definition 3.1.3. For any non-negative integer g, let $d = g + 1$ and $n = g + 3$. Consider the morphism of tropical moduli spaces:

$$F_s \times F_t : \mathscr{H}^{\mathtt{trop}}_{g,d,n} \to \mathscr{M}^{\mathtt{trop}}_{g,n} \times \mathscr{M}^{\mathtt{trop}}_{0,n}. \tag{3.6}$$

After refining the cone complex structures of source and target, we may assume that $F_s \times F_t$ is a strict morphism of generalized cone complexes. We define the **tropical Tevelev degree** to be:

$$\mathsf{Tev}^{\mathtt{trop}}_g := \deg(F_s \times F_t) \tag{3.7}$$

Remark 3.1.4. Definition 3.1.3 makes sense due to the correspondence theorem (Theorem 3.0.1), which shows that the tropical degree equals the well-defined algebraic degree of the map $f_s \times f_t$. It is in fact possible to prove that the degree of the map $F_s \times F_t$ is well-defined directly, combining the perspective and results of [32, 33] with the combinatorial analysis of the map $\mathtt{trop}_\Sigma$ in (3.9). While this approach would be philosophically more satisfying, it is not strictly necessary for our current purpose and it would take us on a significant technical sidetrack, so we omit it.

Remark 3.1.5. With respect to the algebraic definition, we are missing a denominator of $(4g)!$, since we already chose to unmark the legs corresponding to simple branch points in the tropical Hurwitz space.

For later convenience, we describe explicitely how to compute the local degree of the map $F_s \times F_t$ at a point $x = [\phi : \Gamma \to T] \in \mathscr{H}^{\mathtt{trop}}_{g,d,n}$. We refer to (2.11) for the definition of local degree of a map of cone complexes, and to (2.10) for the weights of cones of spaces of tropical admissible covers. For moduli spaces of tropical curves $\mathscr{M}^{\mathtt{trop}}_{g,n}$, maximal cones are weighted by the reciprocal

of the size of the automorphism group of the tropical curves parameterized. We make the following simplifying assumption, which will be true for the covers considered to compute tropical Tevelev degrees:

($\star$) for each edge $e \in T$, there is at most one edge in $\phi^{-1}(e)$ with expansion factor > 1.

Assumption $(\star)$ yields the following two consequences:

1. The last product in (2.10) is equal to 1;
2. for any compact edge e of T, choosing the length of the edge in $\phi^{-1}(e)$ with highest expansion factor (and choosing any one edge if they all have expansion factor 1) as a coordinate for σ_Θ gives us a coordinate system whose integral lattice agrees with the integral structure of σ_Θ.

It follows that the local degree of $F_s \times F_t$ at x is given by:

$$\deg_x(F_s \times F_t) = \frac{|\mathrm{Aut}(\overline{\Gamma})|}{|\mathrm{Aut}(\phi)|} \cdot \prod_{v \in V(\Gamma)} H_v \cdot |\det(M_{\sigma_\Theta})|, \tag{3.8}$$

where M_{σ_Θ} is the matrix whose rows express the lengths of the compact edges of $F_s(\Gamma)$ and $F_t(T)$ as linear functions of the lengths of the edges of Γ chosen as discussed in (2) in the previous paragraph.

We are now ready to prove that the tropical enumerative invariants just defined agree with their algebraic counterparts.

Proof of Theorem 3.0.1. The proof of this theorem is an adaptation of the proof of [24, Theorem 2]; we describe here the necessary modifications and defer to that paper for some of the details that transfer essentially unchanged.

Let $\mathscr{H}^{an}_{g,d,n}$ denote the analytification of the Hurwitz space and by $\Sigma\mathscr{H}^{an}_{g,d,n} \subset \mathscr{H}^{an}_{g,d,n}$ the Berkovich skeleton obtained by compactifying the Hurwitz space by admissible covers. We have a commutative diagram

$$\mathscr{H}^{an}_{g,d,n} \xrightarrow{p} \Sigma\mathscr{H}^{an}_{g,d,n} \xrightarrow{\mathrm{trop}_\Sigma} \mathscr{H}^{\mathrm{trop}}_{g,d,n}, \qquad \mathscr{H}^{an}_{g,d,n} \xrightarrow{\mathrm{trop}} \mathscr{H}^{\mathrm{trop}}_{g,d,n} \tag{3.9}$$

where p is the retraction to the skleleton and the map $\mathtt{trop}_\Sigma$ is a strict morphism of cone complexes which restricts to an isomorphism onto its image for every individual cone, while being globally neither injective nor surjective. Given a maximal dimensional cone $\sigma_\Theta \subset \mathscr{H}^{\mathtt{trop}}_{g,d,n}$ corresponding to a combinatrial type Θ of tropical admissible covers, in [24, Section 4.2.2, Theorem 2] it is shown that there are exactly $w(\Theta)$ cones in $\Sigma\mathscr{H}^{an}_{g,d,n}$ mapping isomorphically onto σ_Θ. Thus making $\mathscr{H}^{\mathtt{trop}}_{g,d,n}$ into a weighted cone complex by giving weight $w(\Theta)$ to each maximal cone σ_Θ makes $\mathtt{trop}_\Sigma$ into a map of weighted cone complexes of degree 1. Now consider the diagram:

$$\begin{array}{ccc}
\mathscr{H}^{an}_{g,d,n} & \xrightarrow{(f_t\times f_s)^{an}} & \mathscr{M}^{an}_{g,n}\times\mathscr{M}^{an}_{0,n} \\
\downarrow{\scriptstyle p} & & \downarrow \\
\Sigma\mathscr{H}^{an}_{g,d,n} & \xrightarrow{f_t\times f_s|_{\Sigma\mathscr{H}}} & \Sigma\mathscr{M}^{an}_{g,n}\times\Sigma\mathscr{M}^{an}_{0,n} \\
\downarrow{\scriptstyle \mathtt{trop}_\Sigma} & & \| \\
\mathscr{H}^{\mathtt{trop}}_{g,d,n} & \xrightarrow{F_t\times F_s} & \mathscr{M}^{\mathtt{trop}}_{g,n}\times\mathscr{M}^{\mathtt{trop}}_{0,n}.
\end{array} \tag{3.10}$$

By the algebraic definition of Tevelev degrees, the map $(f_t \times f_s)^{an}$ is a map of analytic spaces of degree $(4g)!\mathsf{Tev}_g$. The horizontal map in the middle has a somewhat dual nature: it is naturally the restriction to the skeleton of the previous map, giving rise to an analytic map of the same degree; but it is also a map of cone complexes whose combinatorial degree may be computed combinatorially as in Definition 2.7.1. After possibly refining the cone complex structures of source and target we can assume the map to be strict. Let $y = (S,T)$ be a general point in $\Sigma\mathscr{M}^{an}_{g,n}\times\Sigma\mathscr{M}^{an}_{0,n}$, belonging to a maximal cone $\tau_{\overline{\Theta}}$, and $x = \Gamma \to B$ a point in its inverse image in $\Sigma\mathscr{H}^{an}_{g,d,n}$; by the assumption of strictness, x is in the interior of some maximal cone σ_Θ. Combining [34, Section 6] with the fact that both points have isotropy given by the automorphism groups of the tropical objects ((S,T) and $\Gamma \to B$), we obtain that the local analytic degree of $f_t \times f_s|_{\Sigma\mathscr{H}}$ at x is given by

$$\frac{|\mathrm{Aut}(\overline{\Theta})|}{|\mathrm{Aut}(\Theta)|}[\Lambda_{\overline{\Theta}} : \mathrm{Im}(\Lambda_\Theta)],$$

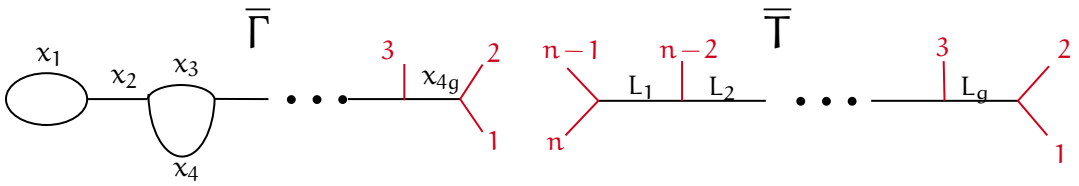

Figure 3.2: The graphs $\overline{\Gamma}, \overline{T}$ defining the chosen point p of $\mathscr{M}_{g,n}^{\mathtt{trop}} \times \mathscr{M}_{0,n}^{\mathtt{trop}}$. The graph $\overline{\Gamma}$, from left to right, consists of a chain of loops, followed by a caterpillar trivalent tree with the marked points in descending order. The x_i's and L_j's label edge lengths, and the legs in red correspond to the marked points. We require $x_i << x_j << \ldots << L_k << L_l$ for $i < j$ and $k < l$, to ensure that p is in the interior of a maximal cone of the refinement of $\mathscr{M}_{g,n}^{\mathtt{trop}} \times \mathscr{M}_{0,n}^{\mathtt{trop}}$ induced by $F_s \times F_t$.

i.e. it agrees with the combinatorial local degree. Finally, since we have given weights to the cones of $\mathscr{H}_{g,d,n}^{\mathtt{trop}}$ to make $\mathtt{trop}_\Sigma$ a map of degree one, we conclude that the combinatorial degree of $F_t \times F_s$ equals the analytic degree of $(f_t \times f_s)^{an}$, which immediately implies $\mathsf{Tev}_g^{\mathtt{trop}} = \mathsf{Tev}_g$.

□

3.2 Computation of tropical Tevelev degrees: proof of Theorem 3.0.2

In this section we exhibit a combinatorial computation for tropical Tevelev degrees. We choose a point $p = (\overline{\Gamma}, \overline{T})$ in the interior of a maximal cone of the refinement of $\mathscr{M}_{g,n}^{\mathtt{trop}} \times \mathscr{M}_{0,n}^{\mathtt{trop}}$ induced by the map $F_s \times F_t$. The pair of tropical curves parameterized by p are depicted in Figure 3.2. We show that $(F_s \times F_t)^{-1}(p)$ consists of 2^g points each of multiplicity one. We start in Section 3.2.1 by computing the tropical Tevelev degrees for three examples in low genera. In Section 3.2.2 we show the construction of 2^g points of multiplicity one for any g. Finally, we end in Section 3.2.3 by ruling out any other points as preimages of the chosen point p.

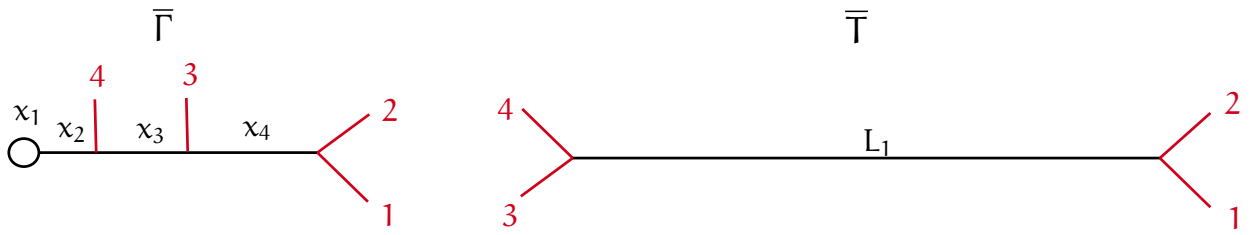

Figure 3.3: The point p in $\mathscr{M}_{1,4}^{\mathrm{trop}} \times \mathscr{M}_{0,4}^{\mathrm{trop}}$. We have $x_1 << x_2 << x_3 << x_4 << L_1$.

3.2.1 Examples in low genera

Base case: $g = 1$**.**

Recalling the set-up from Section 3.1, in order to compute $\mathsf{Tev}_1^{\mathrm{trop}}$ we must compute the degree of the map

$$\mathsf{F_s} \times \mathsf{F_t} : \mathscr{H}_{1,2,4}^{\mathrm{trop}} \to \mathscr{M}_{1,4}^{\mathrm{trop}} \times \mathscr{M}_{0,4}^{\mathrm{trop}}. \tag{3.11}$$

Consider the point $p = (\overline{\Gamma}, \overline{T}) \in \mathscr{M}_{1,4}^{\mathrm{trop}} \times \mathscr{M}_{0,4}^{\mathrm{trop}}$ depicted in Figure 3.3. The set $(\mathsf{F_s} \times \mathsf{F_t})^{-1}(p)$ consists of covers $\phi : \Gamma \to T$ such that T stabilizes to $\overline{T}$ when forgetting the four marked ends with branching data (2), and Γ stabilizes to $\overline{\Gamma}$ when forgetting the four marked ends with expansion factor 2 as well as all the unmarked ends.

Since p lies in the interior of a maximal cone of (an appropriate refinement of) $\mathscr{M}_{1,4}^{\mathrm{trop}} \times \mathscr{M}_{0,4}^{\mathrm{trop}}$, we know that T is a trivalent tree. Forgetting the four marked ends labeled $1,\ldots,4$ and their inverse images, we obtain a cover $\tilde{\phi} : \tilde{\Gamma} \to \tilde{T}$, where $\tilde{T}$ is a trivalent tree with four ends assigned branching data (2). There is exactly one Hurwitz cover of $\tilde{T}$, consisting of two ends with expansion factor one covering the compact edge of $\tilde{T}$ (and forming a loop between two vertices), and two infinite edges with degree 2 coming from each vertex and covering the ends.

We now seek to recover the possible tropical curves Γ by adding four marked points. Since in $\overline{\Gamma}$ the four marked points belong to a tree that attaches to the loop at a trivalent vertex, we conclude that all 4 marked points must belong to the same connected component of Γ minus the loop, i.e. they must all attach to the same infinite edge of degree two. Due to $L_1 >> x_i$ for all i, the cover curve Γ should contain a long edge mapping to the compact edge of $\overline{T}$ that is lost when stabilizing to $\tilde{\Gamma}$. The local description of how the two ways this can happen is depicted in Figure 3.4.

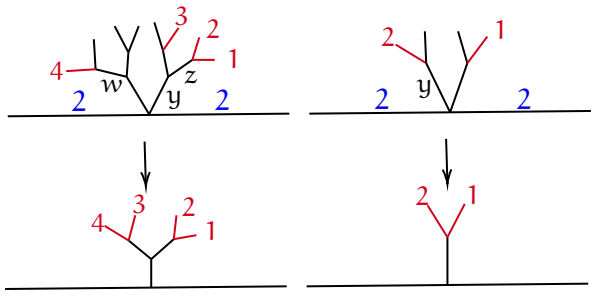

Figure 3.4: A local picture of two configurations of marked points on a degree two tropical cover that allow for a long edge to be forgotten in the stabilization of the cover curve.

Given an edge e of the cover of degree 2, we can attach a trivalent tree to an interior point of $\phi(e)$ (on the base), and then mark ends upstairs as on the left hand side of Figure 3.4. When stabilized, the cover curve no longer has the length w, so w is free to be as long as needed for the compact edge of the base curve to reach length L_1.

The only other option is to attach a tripod with two marked points in an interior point of $\phi(e)$, and then put one marked point on each of the two trees covering the tree in the base, as on the right hand side of Figure 3.4. Now the unique length y is lost in the stabilization of Γ.

From the above local pictures we can get global inverse images of p by placing the marked points on $\tilde{\Gamma}$ to recover Γ in two possible ways. We can attach the tree from the left hand side of Figure 3.4 at distance x_2 from the loop; we can then choose the length $y = x_3, z = x_4, w = L_1 - x_4$.

Alternatively, we place mark 4 at distance x_2 from the loop, followed by mark 3 after a distance of x_3, and finally the marks 2 and 1 on a tripod (as in Figure 3.4) that attaches after distance x_4. We choose $y = L - 2x_4$. Both types of inverse images of p are shown in Figure 3.5.

We now compute the local degree of $(F_s \times F_t)$ at these inverse images, which gives us the multiplicities with which we need to count the covers.

We follow (3.8), and notice that assumption $(\star)$ is verified; hence, for $i = 1, 2$ the multiplicity of the inverse image $\phi_i : \Gamma_i \to T_i$ is the product of three factors: an automorphism factor, a product of local Hurwitz numbers and a dilation factor corresponding to the determinant of the matrix representing the map $F_s \times F_t$.

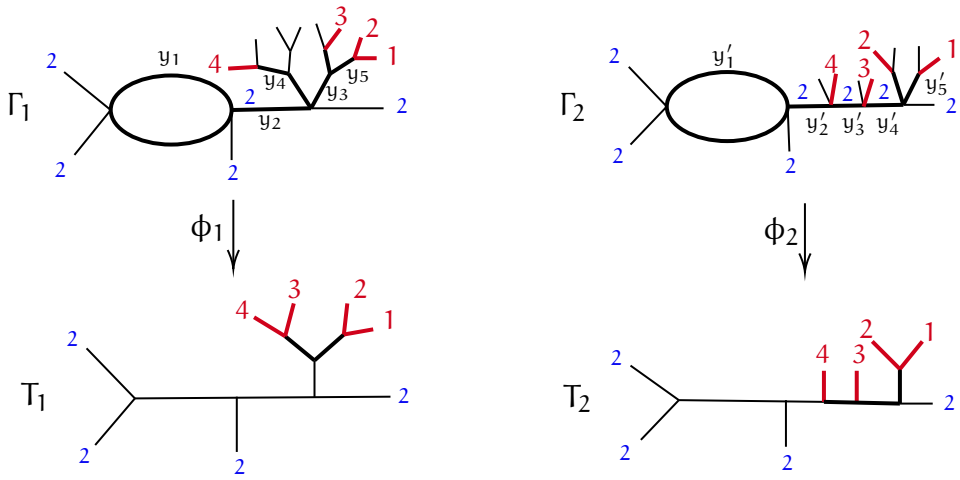

Figure 3.5: The two covers in $(F_s \times F_t)^{-1}(p)$. The thickened parts show the subgraphs to which the graphs stabilize via the maps F_s, F_t.

The automorphism factor is the same for $i = 1, 2$. For each cover, we have $\mathrm{Aut}(\phi_i) = \mu_2 \times \mu_2$: one factor corresponds to switching simultaneously the two unlabeled left ends of branching type 2 and their inverse images; the second factor consists of switching the two degree 1 edges of Γ_i forming the loop. However, this is also a nontrivial automorphism of $\overline{\Gamma_i}$. Altogether, we have

$$\frac{|\mathrm{Aut}(\overline{\Gamma_i})|}{|\mathrm{Aut}(\phi_i)|} = \frac{1}{2}. \tag{3.12}$$

The local Hurwitz numbers factors are also computed identically for $i = 1, 2$: every vertex in the cover is either trivalent with degree one edges in all directions or two edges of degree 2 in different directions and 2 edges of degree 1 in the same direction. Both of these types of vertices have local Hurwitz number equal to 1, therefore the product of all local Hurwitz numbers is 1.

To calculate the dilation factors, we set up the following matrices representing the x_i's and L_j's in terms of the y_k's:

$$M_1 = \begin{array}{c} \\ x_1 \\ x_2 \\ x_3 \\ x_4 \\ L_1 \end{array} \begin{array}{c} \begin{array}{ccccc} y_1 & y_2 & y_3 & y_4 & y_5 \end{array} \\ \begin{bmatrix} 2 & 0 & 0 & 0 & 0 \\ 0 & 1 & 0 & 0 & 0 \\ 0 & 0 & 1 & 0 & 0 \\ 0 & 0 & 0 & 0 & 1 \\ 0 & 0 & 0 & 1 & 1 \end{bmatrix} \end{array} \quad M_2 = \begin{array}{c} \\ x_1 \\ x_2 \\ x_3 \\ x_4 \\ L_1 \end{array} \begin{array}{c} \begin{array}{ccccc} y_1' & y_2' & y_3' & y_4' & y_5' \end{array} \\ \begin{bmatrix} 2 & 0 & 0 & 0 & 0 \\ 0 & 1 & 0 & 0 & 0 \\ 0 & 0 & 1 & 0 & 0 \\ 0 & 0 & 0 & 1 & 0 \\ 0 & 0 & 0 & 1 & 1 \end{bmatrix} \end{array}$$

We see that $|\det M_i| = 2$ for $i = 1, 2$. All together the multiplicity of each cover in $(\mathsf{F_s} \times \mathsf{F_t})^{-1}(p)$ is $1 \cdot \frac{1}{2} \cdot 2 = 1$. Since we have two inverse images each with multiplicity one, we obtain $\mathsf{Tev}_1^{\mathtt{trop}} = 2$.

Low genus examples: $g = 2$**.**

To compute $\mathsf{Tev}_2^{\mathtt{trop}}$, we look for the degree of the map

$$\mathsf{F_s} \times \mathsf{F_t} : \mathscr{H}_{2,3,5}^{\mathtt{trop}} \to \mathscr{M}_{2,5}^{\mathtt{trop}} \times \mathscr{M}_{0,5}^{\mathtt{trop}}. \tag{3.13}$$

We consider the point $p = (\overline{\Gamma}, \overline{\mathsf{T}}) \in \mathscr{M}_{2,5}^{\mathtt{trop}} \times \mathscr{M}_{0,5}^{\mathtt{trop}}$ as illustrated in Figure 3.2. With notation as in the previous section, we know that $\tilde{\mathsf{T}}$ is a trivalent tree, but unlike the genus 1 case, there are multiple options for how this tree can be shaped. For two of these $\tilde{\mathsf{T}}$-trees it is possible to place fragments of the marked tree $\overline{\mathsf{T}}$ to obtain the base T of the cover.

When adding the 5 marked points, we use the same techniques as in the previous section to get two long edges of Γ that map to compact edges of $\overline{\mathsf{T}}$ and are lost when stabilizing to $\overline{\Gamma}$. All of the preimages are shown in Figure 3.6.

We can now find the multiplicities of these covers by computing the local degree of $(\mathsf{F_s} \times \mathsf{F_t})$ at all 4 inverse images. The automorphism factor is the same for all 4. For each cover, there are two pairs of ends of branching type 2 that can be switched, corresponding to the first two forks

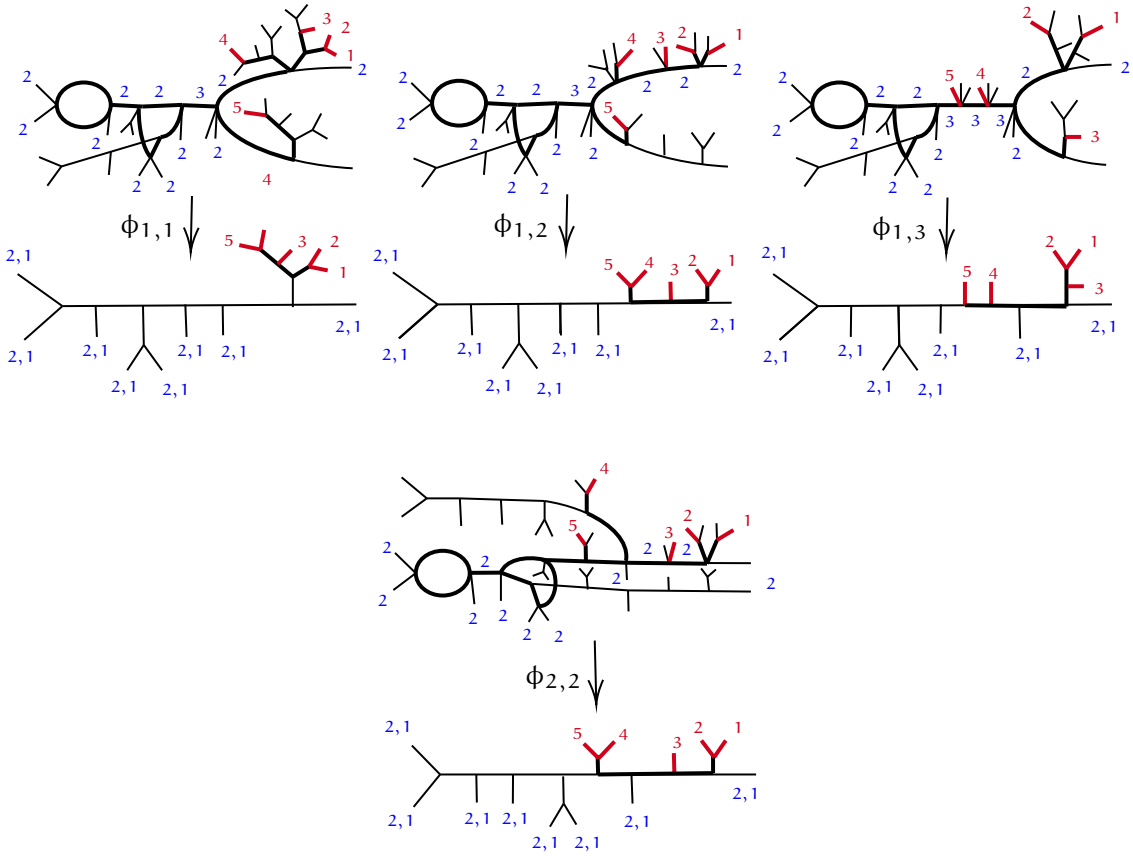

Figure 3.6: The four covers in $(F_s \times F_t)^{-1}(p)$ when $g = 2$. The thickened parts show the subgraphs to which the graphs stabilize via the maps F_s, F_t.

starting from the left side of the base cover; these give 4 automorphisms of ϕ that are not also automorphisms of $\overline{\Gamma}$. The product of local Hurwitz numbers for all covers is equal to 1, recall Convention 3.1.2.

The matrices that compute the multiplicities for these inverse images are written in Figure 3.7. All four matrices are block diagonal and have absolute value of the determinant equal to 4, therefore all four covers have multiplicity $\frac{4}{4} = 1$, and we get $\mathsf{Tev}_2^{\mathtt{trop}} = 4$.

Low genus examples: $g = 3$**.**

For our final example, consider the point $p = (\overline{\Gamma}, \overline{T}) \in \mathscr{M}_{3,6}^{\mathtt{trop}} \times \mathscr{M}_{0,6}^{\mathtt{trop}}$ shown in Figure 3.2. There are eight preimages as shown in Figure 3.8, each has multiplicity 1, so $\mathsf{Tev}_3^{\mathtt{trop}} = 8$.

$$M_{1,1} = \left[\begin{array}{cccc|cccccc} 2&0&0&0&0&0&0&0&0&0\\ 0&1&0&0&0&0&0&0&0&0\\ 0&0&1&0&0&0&0&0&0&0\\ 0&0&2&2&0&0&0&0&0&0\\ \hline 0&0&0&0&1&0&0&0&0&0\\ 0&0&0&0&0&1&0&0&0&0\\ 0&0&0&0&0&0&1&0&0&0\\ 0&0&0&0&0&0&0&1&0&0\\ 0&0&0&0&0&0&0&0&1&0\\ 0&0&0&0&0&0&0&1&1&0 \end{array}\right] \quad M_{1,2} = \left[\begin{array}{cccc|cccccc} 2&0&0&0&0&0&0&0&0&0\\ 0&1&0&0&0&0&0&0&0&0\\ 0&0&1&0&0&0&0&0&0&0\\ 0&0&2&2&0&0&0&0&0&0\\ \hline 0&0&0&0&1&0&0&0&0&0\\ 0&0&0&0&0&1&0&0&0&0\\ 0&0&0&0&0&0&1&0&0&0\\ 0&0&0&0&0&0&0&1&0&0\\ 0&0&0&0&0&0&1&2&0&0\\ 0&0&0&0&0&0&0&0&2&1 \end{array}\right] \quad M_{1,3} = \left[\begin{array}{cccc|cccccc} 2&0&0&0&0&0&0&0&0&0\\ 0&1&0&0&0&0&0&0&0&0\\ 0&0&1&0&0&0&0&0&0&0\\ 0&0&2&2&0&0&0&0&0&0\\ \hline 0&0&0&0&1&0&0&0&0&0\\ 0&0&0&0&0&1&0&0&0&0\\ 0&0&0&0&0&0&1&0&0&0\\ 0&0&0&0&0&0&0&1&0&0\\ 0&0&0&0&0&0&3&2&1&0\\ 0&0&0&0&0&0&0&0&0&1 \end{array}\right]$$

$$M_{2,2} = \left[\begin{array}{cccc|cccccc} 2&0&0&0&0&0&0&0&0&0\\ 0&1&0&0&0&0&0&0&0&0\\ 0&0&1&0&0&0&0&0&0&0\\ 0&0&1&2&0&0&0&0&0&0\\ \hline 0&0&0&0&1&0&0&0&0&0\\ 0&0&0&0&0&0&1&0&0&0\\ 0&0&0&0&0&0&0&1&0&0\\ 0&0&0&0&0&0&0&0&1&0\\ 0&0&0&0&0&1&1&2&0&0\\ 0&0&0&0&0&0&0&0&2&1 \end{array}\right]$$

Figure 3.7: The matrices computing the local degree of $(F_s \times F_t)$ at the four inverse images of p. We observe that the matrices are block diagonal, with one block having determinant a power of 2 and the other determinant one.

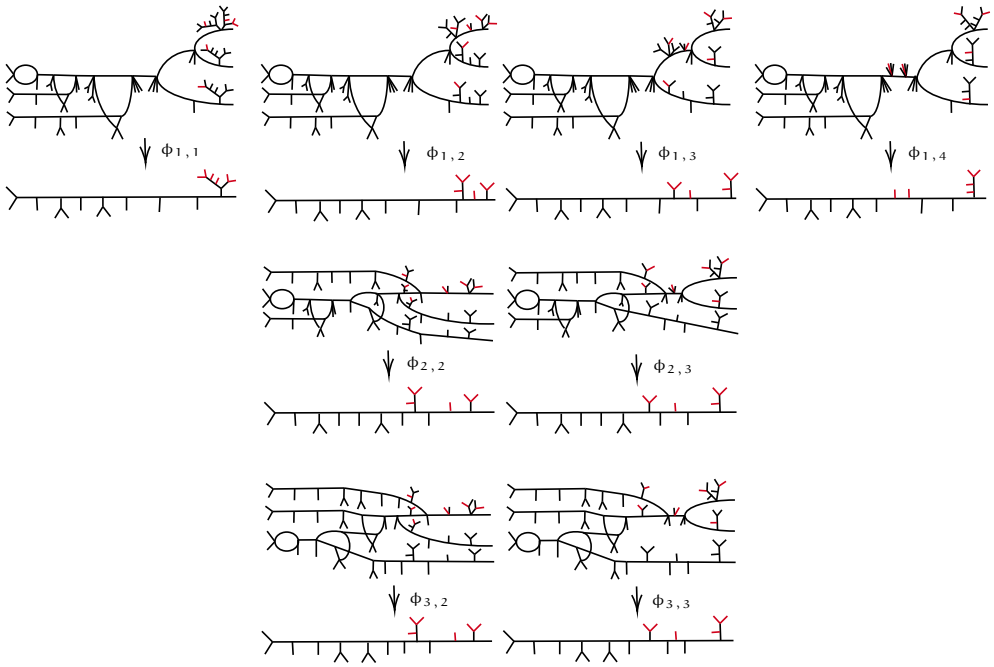

Figure 3.8: Genus 3 covers contributing to $\mathsf{Tev}_3^{\mathtt{trop}}$

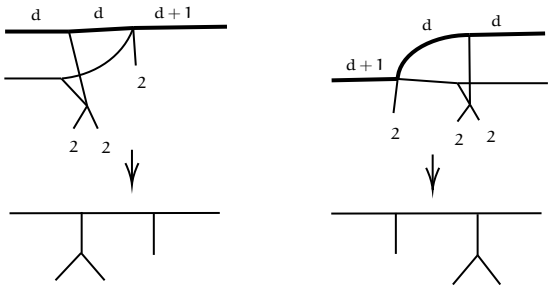

Figure 3.9: Two possible ways to add genus. We omit from the picture ends of degree 1 to avoid clutter. The active path is thickened. We remark that the two fragments are just the reflection of one another about a vertical axis, but the two distinct directions play an important role in our story.

3.2.2 Construction of 2^g solutions

In this section we make explicit and generalize the constructions from the examples in Section 3.2.1, and construct 2^g preimages of p for any genus g. We organize the task into four parts: in Section 3.2.2 we build a cover containing all the genus and no marked points (we call it the genus part of the cover and denote it by $\widehat{\Gamma} \to \widehat{T}$); in Section 3.2.2 we construct a tree containing the n marked ends that attaches to the genus part of Γ, which we call the marked tree part of the cover. In Section 3.2.2 we show that the multiplicity of every cover constructed is equal to 1. We conclude in Section 3.2.2 by organizing the combinatorics of the problem and show we have constructed 2^g covers contributing to Tev_g.

The genus part

For any integer $d \geq 1$, we consider the two tropical covers of degree $d+1$ depicted in Figure 3.9, which we call U and D, and together we call *genus fragments*. The base of each cover is a trivalent tree with five ends. We think of this tree as an oriented line to which we attach one simple end and a tripod, in the two possible orders. The cover curves are connected genus one tropical curves; for every horizontal end/edge of the base curve there is a unique end/edge in the cover mapping to it with degree greater than one; we call it the *active end/edge* and we call the collection of all active ends/edges the *active path*. In the case of fragment D when $d = 1$, we choose an arbitrary connected lift of the horizontal path of the base curve and declare it to be the active path.

Notice that in the two cases the degree of the active path either goes up or down by one after making the genus.

For any genus $g \geq 2$, we construct (topological types of) tropical covers of genus g, degree $d \leq g+1$ as follows:

1. Start with the unique degree 2, genus one cover of a trivalent, four ended tree as in Section 3.2.1; choose any one of the four ends to be the active edge;

2. attach a sequence of $g-1$ genus fragments by gluing the rightmost horizontal end of the base graph to the leftmost end of the next graph, and gluing the corresponding active edges above. Observe that the fragment U can always be used, whereas the fragment D can be used whenever the degree of the attaching active end is greater than one.

3. complete the resulting graphs with appropriate portions of degree 1 to make it into an honest global cover of tropical curves. This can be always done in a unique way.

If the fragment D has been used i times we obtain a connected cover of degree $g+1-i$ with active end of degree $g+1-2i$. We complete it to a degree $g+1$ cover by adding i disjoint copies of the base curve each mapping with degree one.

We conclude this section with the elementary observation that for all covers thus constructed the degree of the active end has the same parity as $g+1$.

We have constructed tropical covers containing all the genus and none of the marked points needed: we call these covers the *genus part* of our solutions and denote them by $\widehat{\Gamma} \to \widehat{T}$.

The marked tree part

Given a cover $\Gamma \to T$, we denote by $\tilde{\Gamma} \to \tilde{T}$ the cover obtained by forgetting the n marked points. For any genus part of a cover $\widehat{\Gamma} \to \widehat{T}$ constructed in the previous section, the degree of the active end can be any positive number congruent to d modulo 2. Given a genus part with active edge of degree $d-2i$, we show first how to complete it to unmarked covers $\tilde{\Gamma} \to \tilde{T}$; next we add further trees containing the (images of the) marked points to $\tilde{T}$ to obtain T; finally we describe the inverse images of these trees and describe how to place the marked points on them.

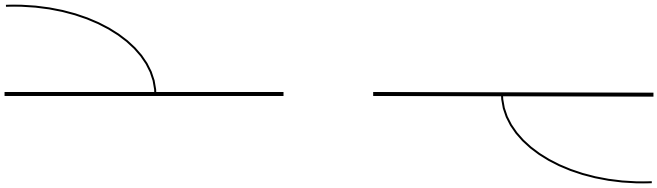

Figure 3.10: The active edge, drawn thickened, is oriented from left to right, i.e. away from the genus part. An edge joining the active edge is shown on the left, and an edge cutting from the active edge is shown on the right.

Cuts and joins: constructing $\tilde{\Gamma} \to \tilde{T}$

For any genus part of a cover, we complete $\widehat{T}$ to $\tilde{T}$ by extending horizontally the end that the active edge maps to and attaching to it $g-1$ vertical ends. Together with the final horizontal end, we have added g simple branched ends to $\widehat{T}$ and therefore obtained a good candidate for $\tilde{T}$. A consequence of the simple branching conditions is that for any cover of $\tilde{\Gamma} \to \tilde{T}$, the inverse image of the horizontal edge of $\tilde{T}$ must be a trivalent tree, hence it should be obtained from the active edge by a series of *cuts and joins* (illustrated in Figure 3.10).

Consider a genus part $\widehat{\Gamma} \to \widehat{T}$ where the active edge has degree d: then we obtain a unique cover $\tilde{\Gamma} \to \tilde{T}$ by a sequence of cuts where one of the ends has expansion factor equal to 1, and the other (of degree greater than one) is the new *active edge*. We call the sequence of active edges the *active path*. Observe that since we have $g-1$ cuts, the final active end has degree $d-(g-1)=2$, and is therefore a simply ramified end, as required. We observe that since all the non-active ends have degree 1, there is a unique way to extend them to a cover of the portion of the tree $\tilde{T}$ that they must cover.

For $1 \leq i \leq \lfloor \frac{d-1}{2} \rfloor$, we complete the genus part $\widehat{\Gamma}_i \to \widehat{T}_i$ in $d-2i$ different ways: informally, the idea is that we keep all the joins together. Formally, for $0 \leq k \leq d-2i-1$, we denote by $\tilde{\Gamma}_{i,k} \to \tilde{T}_{i,k}$ the cover where the active path consists of k cuts, followed by i joins, followed by the remaining cuts, as illustrated in Figure 3.11. We remark again that for each of the degree one edges emanating from the active path, there is a unique way to complete them to a degree one cover of the portion of $\tilde{T}$ they must cover.

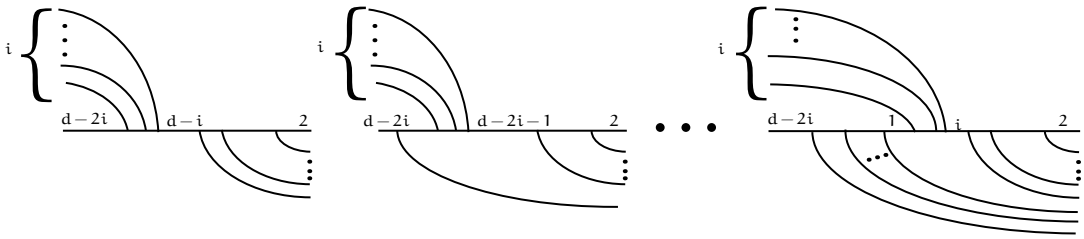

Figure 3.11: The sequence of cuts and joins admitted for a given i.

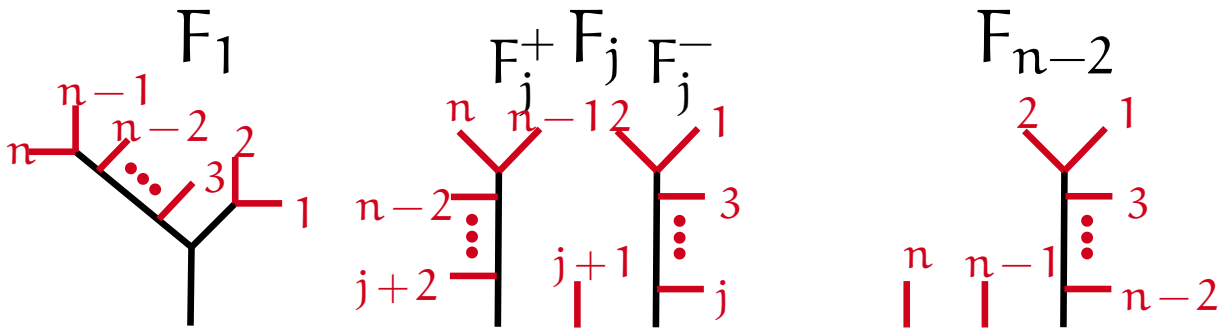

Figure 3.12: Marked fragments that attach to the horizontal edge of $\tilde{T}$ to obtain the base graph T. We denote by F_j^- the connected component that contains the marks with the lowest indices, and F_j^+ the one containing the highest labels.

The marking fragments

In the next section, we will construct T from $\tilde{T}$ by attaching to the horizontal edge of $\tilde{T}$ one of the $(n-2)$ marked fragments depicted in Figure 3.12. Note that since we are in the base cover, the marks are really representing the images of the marks. Finally observe that F_1 contains the tree $\overline{T}$; for $1 \leq j \leq n-3$, the tree $\overline{T}$ is formed by the fragment together with the portion of the horizontal edge of $\tilde{T}$ between the two outer connected components of the fragment. For $j = n-2$, when stabilizing, the n-th marked end will be adjacent to the $(n-1)$-th at a vertex v, and $\overline{T}$ will consist of these two ends, the portion of the horizontal edge from v to the remaining part of the fragment, and the remaining part of the fragment. For now, we don't discuss how the connected components of the fragments are positioned with respect to the simple branched ends stemming from the horizontal edge of $\overline{T}$. We will discuss the various possible cases when we describe the inverse images of the fragments to construct the cover Γ.

Constructing the covers

In this section we construct covers $\Gamma \to T$ in $(F_s \times F_t)^{-1}(p)$. Given a genus part of the cover ending with an active edge of degree $d-2i$ and a fragment F_j with

$$i \le j \le n-2-i = d-i, \tag{3.14}$$

we show how to attach F_j to $\tilde{T}$ to obtain T, and how to mark the inverse images of the fragment to obtain the cover Γ. We discuss several cases.

CASE 1: $i > 0$. Given a genus part with active edge of degree $d-2i$ and j in the range specified in (3.14), we complete the genus part to a cover of type $\tilde{\Gamma}_{i,k} \to \tilde{T}_{i,k}$ as described in Section 3.2.2, for $k = d-i-j$. We first describe the topological type of the cover, and then concern ourselves with the metric information. Refer to Figure 3.13 to follow the various constructions involved.

Pick three points on the (image of the) active path[2]:

q^+ on the $(k+1)$-th edge of the active path, separating the first set of cuts from the joins;

q^0 on the $(i+k+1)$-th edge of the active path, separating the joins from the remaining cuts;

q^- on the last edge of the active path.

To obtain $T_{i,k}$, we attach F_j^+ to the point q^+, the (image of the) marked point $j+1$ to q^0 and F_j^- to the point q^-.

For $\Gamma_{i,k}$, we mark the points in the inverse images of F_j as follows:

1. Order the (connected components of the) inverse images of F_j according to the order of their closest point to the active path;
2. place the mark n on the first inverse image of F_j^+
3. Place all marks > 2 in descending order one on each consecutive inverse image of (the appropriate connected component of) F_j.

[2]Since we are concerned only with the tree part of the cover, we now start counting the edges of the active path from right after the last loop is closed.

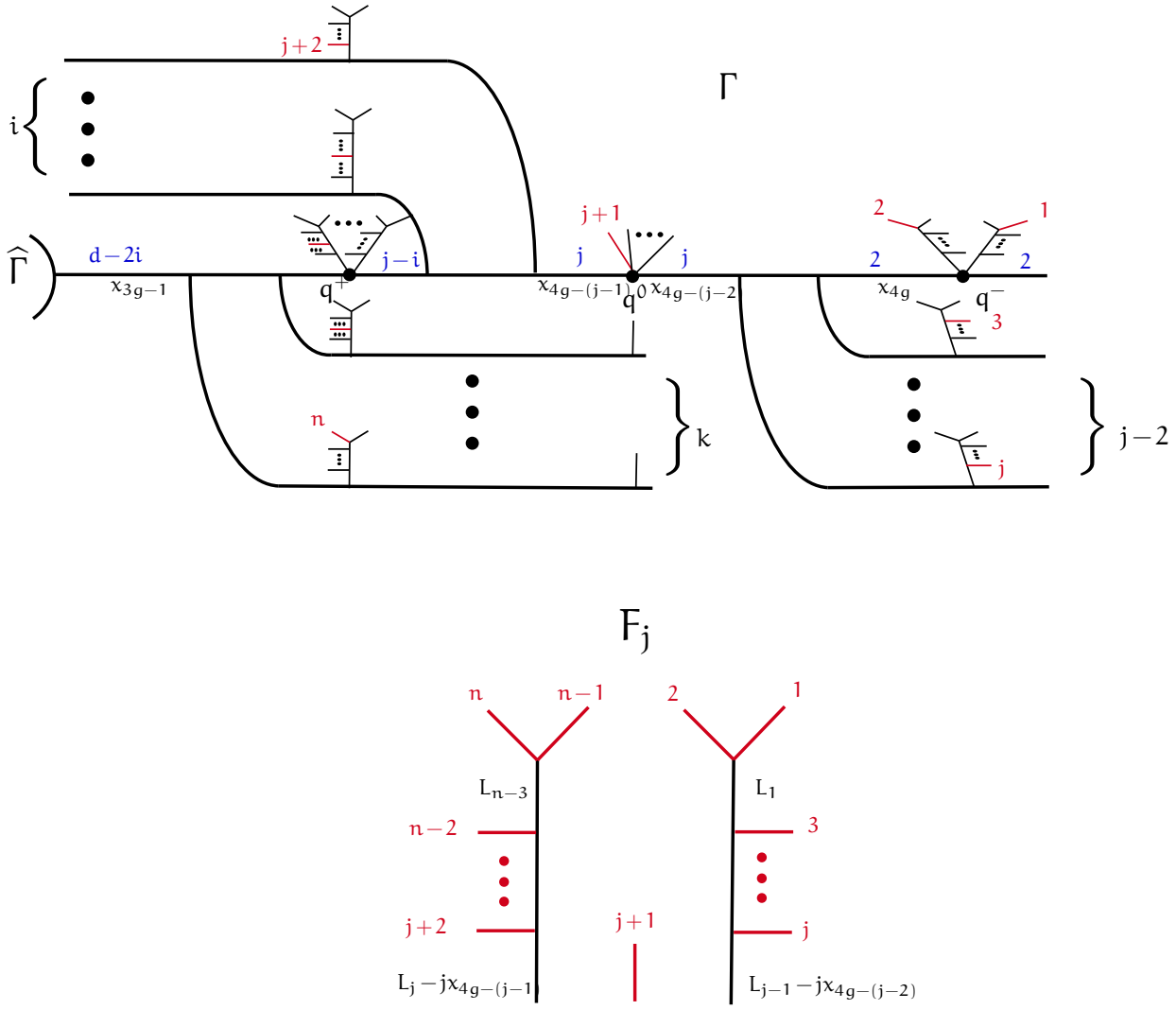

Figure 3.13: The top part of the picture represents the tree part of the cover $\phi_{i,j}$ for $i \neq 0$. The inverse images of the points $q^{\pm}, q^0$ on the active path are still denoted by the same names to not clutter the picture. The metric information for the fragment F_j is depicted in the bottom part of the picture as it would not fit above: since all connected components of the inverse image of F_j have local degree one, the lengths are the same in the top graph.

4. Place the marks $1,2$ on the last inverse image of F_j^-, making sure that the two marks are on distinct branches of such inverse image: note that since the point q^- lies on an edge of degree 2, the inverse image of F_j^- consists of two copies of F_j^-.

We now proceed to describe the metric information. The active path contains $(g+2)$ edges: give the first one length x_{3g-1}, and each successive length of $\overline{\Gamma}$ until x_{4g}.

For all edges of the fragment F_j, except the two bottom edges of $F_j^{\pm}$, give them the length L_i of the corresponding edge in $\overline{T}$. The bottom edge of F_j^- is given length $L_{j-1} - jx_{4g-(j-2)}$, and the bottom edge of F_j^+ is given length $L_j - jx_{4g-(j-1)}$. We have thus constructed a cover in the inverse image of p which we call $\phi_{i,j}$.

CASE 2: $i = 0, j > 1$. This case is illustrated in Figure 3.14. When $i = 0$, i.e. the genus part of the cover ends with an active edge of degree d, the only option for the cover $\tilde{\Gamma}_{1,j} \to \tilde{T}_{1,j}$ is to be formed by a sequence of $g-1$ cuts from the active edge.

To obtain the (topological type of the) base graph $T_{1,j}$, mark two points q^+, q^0, in this order, on the edge after $(n-2-j)$ cuts; place a mark q^- on the last edge of the active path. Attach the fragments $F_j^{\pm}$ to the points $q^{\pm}$ and the mark $j+1$ to the point q^0. On the cover graph, the marks are placed on the inverse images of the fragments in descending order as you proceed along the active path. As in the previous case, the marks 1 and 2 should be on distinct branches of the inverse image of F_j^-. The metric information is also analogous to the previous case, and it is illustrated in Figure 3.14.

CASE 3: $i = 0, j = 1$. This case is illustrated in Figure 3.15. Again, the base cover is obtained by performing a sequence of cuts on the active edge. We mark one point on the last edge of the active path, and attach the fragment F_1 to it. On the cover curve, the marks are placed one on each connected component of the inverse image of F_1 in descending order, so that the mark n will stabilize to the vertex of the first cut, and so on. The last connected component of the inverse image of F_1 attaches to a degree 2 edge, and therefore consists of two copies of the fragment F_1. We mark the point 4 on one copy, and the points $3,2,1$ on the other.

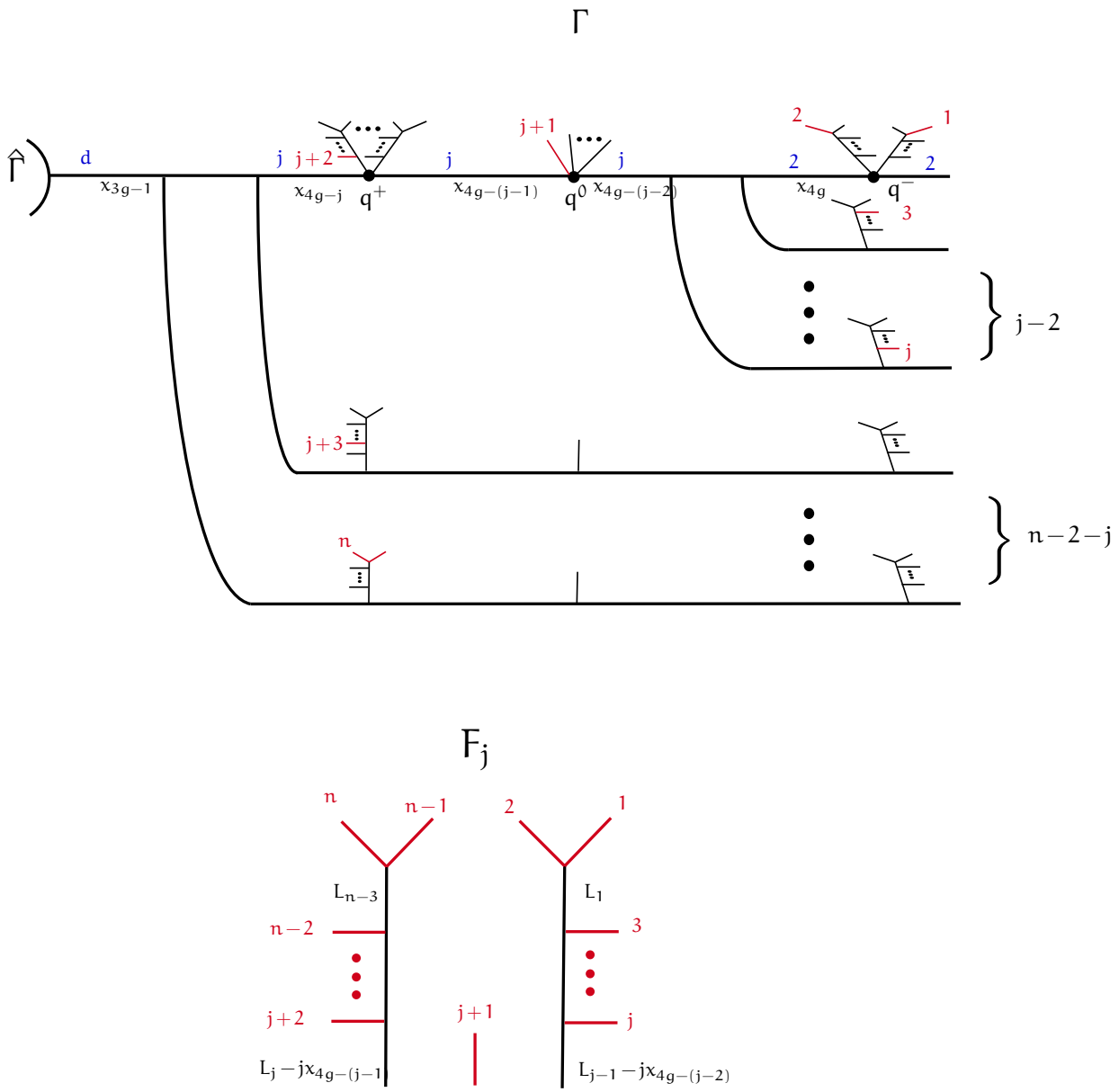

Figure 3.14: The top part of the picture represents the tree part of the cover $\phi_{i,j}$ for $i = 0, j \neq 1$. The metric information for the fragment F_j is depicted in the bottom part of the picture.

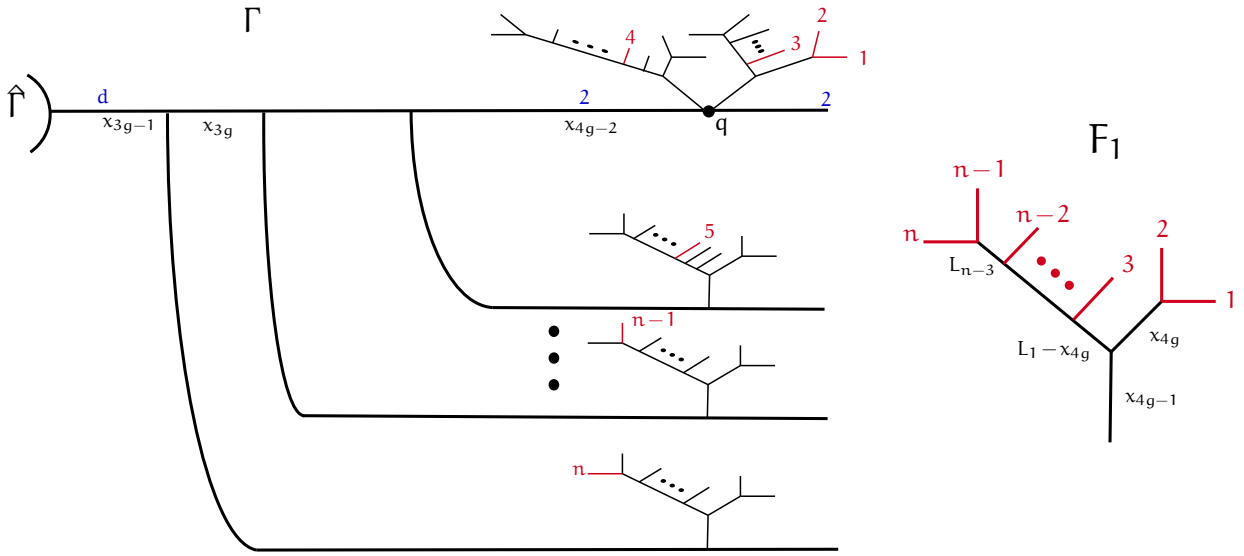

Figure 3.15: The left part of the picture represents the tree part of the cover $\phi_{i,j}$ for $i = 0, j = 1$. The metric information for the fragment F_1 is depicted on the right part of the picture.

As for the metric information, consider the path from $\widehat{\Gamma}$ to the vertex supporting the marks $1, 2$, and give the edges of this path lengths $x_{3g-1}, \ldots, x_{4g}$. The remaining edges of the fragment are given lengths $L_1 - x_{4g}, L_2, \ldots, L_{n-3}$ as depicted in Figure 3.15.

Multiplicities

In this section we compute the local degree of the map $F_s \times F_t$ at each of the inverse images of the point p, giving the multiplicities we need to count the covers constructed. Following (2.6), the local degree is the product of three factors: an automorphism factor, a local Hurwitz numbers factor, and a dilation factor.

There are two types of local Hurwitz numbers appearing in the graphs constructed: either numbers of the form $H_0(\alpha, (2, 1^{d-2}), \beta)$, or of the form $H_0((d), (d), 1)$, where this notation means that the third point on the base is not a branch point, but only one of its inverse images is marked (see Convention 3.1.2). Both these types of Hurwitz numbers are equal to one, and therefore the Hurwitz number factor is also equal to one.

The dilation factor equals the determinant of the matrix M_g giving the local expression for the map $F_s \times F_t$; call x_i, L_j the lengths of the edges of the graphs $\overline{\Gamma}, \overline{T}$, and y_k the lengths of $5g$ edges

of Γ chosen as in observation (2) after condition $(\star)$; then the rows of the matrix express the y_k's as linear functions of x_i, L_j. Since all covers can be split into a genus part and a marked tree part, the matrix used to calculate the dilation factor is block diagonal. The block corresponding to the genus part has size $3g-2$, the other block has size $2g+2$.

Claim 3.2.1. The determinant of the marked tree block equals one.

Proof. The following two facts are used to calculate the determinant of this block. First, all marked points stabilize to the active path, so for $i \geq 3g-1$ the rows corresponding to x_i's contain exactly one non-zero entry, which is in fact equal to 1. We can therefore eliminate the rows and columns containing these entries. Next, when writing the lengths L_i's in terms of the lengths y_j's, we observe that there is exactly one length of the cover that contributes to L_i and does not lie on the active path. Recall that each cover has one free length for every L_i, and the corresponding entry is 1. These two facts together give that the absolute value of the determinant is one. □

Claim 3.2.2. The determinant of the block corresponding to the genus part of the cover is equal to 2^g.

Proof. The block that corresponds to the genus part of the cover is itself made of smaller blocks. We assign the following matrices, M_U and M_D, respectively, to the genus fragments U and D.

$$M_U = \begin{bmatrix} 1 & 0 \\ d & 2 \end{bmatrix} M_D = \begin{bmatrix} 1 & 0 \\ d-1 & 2 \end{bmatrix}$$

The genus block of the matrix is constructed as a sequence of 1×1 and 2×2 diagonal blocks as follows. There is an initial diagonal entry of 2 corresponding to the first loop. Then we have a block diagonal entry of M_U or M_D depending on which type of genus fragment has been used to form the second genus. Between every loop there is an edge that is part of the active path and thus there is a 1 on the diagonal between any two consecutive M_U/M_D blocks. In conclusion, we have $g-1$ (2×2)-blocks of determinant 2, one diagonal entry of 2 and $g-1$ more diagonal entries of 1, and the claim follows. □

Finally, we show that the determinant of the matrix M_g equals the automorphism factor. The automorphisms of the cover that do not pull back from automorphisms of $\overline{\Gamma}$ correspond to switching pairs of simple branch points attached to the same vertex and their preimages. There is one such pair attached to the first loop, and one for each genus fragment, corresponding to the two ends of the attached tripod. All together, $|\mathrm{Aut}(\phi)|/|\mathrm{Aut}(\overline{\Gamma})| = 2^g$.

Putting everything together, for any point x corresponding to a genus g Hurwitz cover ϕ that we have constructed,

$$\deg_x(F_s \times F_t) = \frac{|\mathrm{Aut}(\overline{\Gamma})|}{|\mathrm{Aut}(\phi)|} \cdot |\det(M_g)| \cdot \prod_{v \in V(\Gamma)} H_v = \frac{1}{2^g} \cdot 2^g \cdot 1 = 1.$$

Counting solutions

We now organize the covers constructed in a way that allows us to count them. We put the covers $\Gamma \to T$ inside (but not filling) a rectangular array, where the rows correspond to solutions with the same genus part, and the columns to covers with the same marked fragment type. We order the rows so that the degree of the active edge is non-increasing, and we order the marked fragments by the index j as in Figure 3.12. It is immediate that this table has $n-2$ columns, while it takes a bit of care to count the number of rows.

Each genus part of a cover corresponds to a word of length $g-1$ in the letters U and D, subject to the condition that at every step the degree of the active end remains positive. There is a natural bijection, illustrated in Figure 3.16, between genus parts of the cover and plane paths made by concatenating $g-1$ vectors of type $U = (1,1)$ or $D = (1,-1)$, starting at the point $(1,2)$ and never going below the $y = 1$ line. In particular, the y-coordinate of the endpoint of a path corresponds precisely to the degree of the resulting active end.

While it is not immediate (at least to us) how to count the number of paths with a given endpoint, it is rather simple to count paths with endpoint of the form (g,y) with (g,y_0) fixed and $y \geq y_0$; letting $y_0 = d-2i$ this counts the number of genus parts of covers with active end greater or equal than $d-2i$.

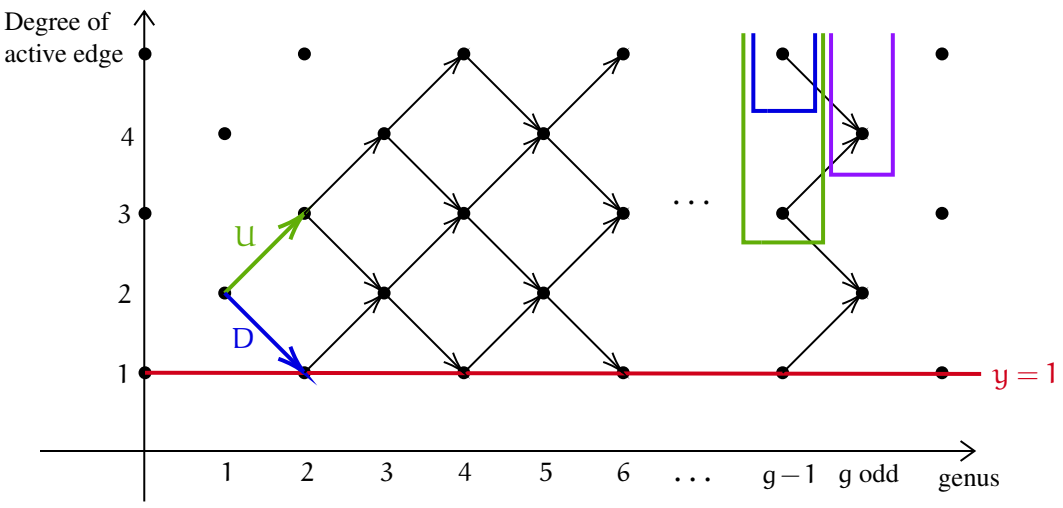

Figure 3.16: A graph showing for each g which degrees are possible for the active edge by adding U or D, green or blue arrow, respectively. The green, blue, and purple boxes demonstrate the proof of Lemma 3.2.3.

Lemma 3.2.3. *For* $d = g+1 \geq 2$, $0 \leq i \leq \lfloor \frac{d-1}{2} \rfloor$, *denote by* $A_{d,\geq d-2i}$ *denote the number of paths described above with endpoint of coordinate* (d, y), $y \geq d-2i$.

$$A_{d,\geq d-2i} = \binom{d-1}{i}. \tag{3.15}$$

Proof. The statement is true by inspection for $d = 2$. Next, partition paths in $A_{d,\geq d-2i}$ by the type of the last step. Those with last step U are naturally in bijection with $A_{d-1,\geq d-2i-1}$, and those with last step D are naturally in bijection with $A_{d-1,\geq d-2i+1} = A_{d-1,\geq d-1-2(i-1)}$; inducting on d we obtain

$$A_{d,\geq d-2i} = \binom{d-2}{i} + \binom{d-2}{i-1} = \binom{d-1}{i}. \tag{3.16}$$

□

In Section 3.2.2 we showed that for every genus part of a cover with active edge $d-2i$ we could complete it to a cover with marked fragment type F_j with $i \leq j \leq n-2-i$. Counting the solutions by columns, we see that the columns corresponding to F_j has exactly $A_{d,\geq d-j-1}$ covers. Recalling

$d = g+1 = n-2$, we obtain:

$$|(F_s \times F_t)^{-1}(p)| = \sum_{j=1}^{d} A_{d,\geq d-j-1} = \sum_{m=0}^{d-1} \binom{d-1}{m} = 2^{d-1} = 2^g. \tag{3.17}$$

Since we showed in Section 3.2.2 that each cover counts with multiplicity equal to one, we have thus far shown that $\mathsf{Tev}_g \geq 2^g$. In the next section we complete the proof of Theorem 3.0.2 by excluding the possibility of any further contributing cover.

3.2.3 Excluding further solutions

In this section, we exclude any further cover $\Gamma \to T$ from mapping to the chosen point $p = (\overline{\Gamma}, \overline{T}) \in \mathscr{M}_{g,n}^{\mathtt{trop}} \times \mathscr{M}_{0,n}^{\mathtt{trop}}$. We do this by showing no other marked fragments work, there is no other way to form a genus part of the cover with independent cycle lengths, and all joins on Γ must occur in a row.

Fragments attaching to the active edge

We begin by introducing some notation. Consider a cover $\phi : \Gamma \to T \in (F_s \times F_t)^{-1}(p)$.

We call the path connecting the last cycle of Γ with the vertex in Γ to which the ends marked 1 and 2 stabilize in $\overline{\Gamma}$ the *active path* of Γ, and denote it by $AP(\Gamma)$. While the stabilization function $T \to \overline{T}$ does not typically admit a global continuous section, such section exists when restricting our attention just to the compact edges of $\overline{T}$. We call this section $\sigma_{\overline{T}} : E(\overline{T}) \to T$.

Lemma 3.2.4. *The intersection*

$$\mathrm{Im}(\sigma_{\overline{T}}) \cap \phi(AP(\Gamma)) \tag{3.18}$$

does not contain the entire image of any edge of $\overline{T}$.

Proof. One of the aspects of the chosen point p is that the lengths L_i in $\overline{T}$ are all much longer than the lengths in $\overline{\Gamma}$. The length of the active path in Γ equals the sum of the lengths $x_{3g-1} + \ldots + x_{4g}$, and therefore the length of its image is bounded by $d \cdot (x_{3g-1} + \ldots + x_{4g})$, which is by construction less than any of the L_i, thus proving the Lemma. □

Since the marked ends stabilize to the active path, it must be that the intersection (3.18) is non-empty, and because the base tree is trivalent it must be an interval with nonempty interior. Further, (3.18) must consist either of an interval of an external edge of $\sigma_{\overline{\Gamma}}(\overline{T})$, or an interval containing a marked end; if (3.18) were only a part of a single interior edge e_i of $\sigma_{\overline{\Gamma}}(\overline{T})$, by varying the lengths of the two edges in Γ adjacent to the intersection one would obtain infinitely many distinct graphs giving length L_i to the stabilization of the edge e_i, which is not possible because the point p has been chosen to be in the interior of a maximal cone of (the refinement of) the product $\mathscr{M}_{g,n}^{\mathtt{trop}} \times \mathscr{M}_{0,n}^{\mathtt{trop}}$. It follows from this discussion that, after reintroducing the marked ends, the complement $\mathrm{Im}(\sigma_{\overline{\Gamma}}) \smallsetminus \phi(AP(\Gamma))$ must be one of the $n-2$ fragments described in Section 3.2.2.

Splitting of transpositions

We recall that the graph $\widetilde{T}$, obtained by forgetting the images of the marked points, has $4g$ ends, all corresponding to simple branched ends for the tropical cover. Borrowing language from the monodromy representation of a Hurwitz cover, we call *transpositions* the collection of ends above a branched end which attach to a vertex v with local degrees $2, 1^{d_v-2}$. As we remarked in Section 3.2.2, removing the simple transpositions and unramified parts of the cover leaves us with a trivalent graph from which the entire cover can be uniquely recovered. In what follows we refer to this trivalent graph, and relevant parts of it, by the names $\Gamma, \widetilde{\Gamma}, \widehat{\Gamma}$. We first analyze how the $4g$ transpositions are split between $\widehat{\Gamma} \to \widehat{T}$ and the rest of $\Gamma \to T$.

Claim 3.2.5. The genus part of the graph $\widehat{\Gamma} \to \widehat{T}$ contains at least $3g$ transpositions.

Proof. By the Riemann-Hurwitz formula, the smallest number of transpositions to make a graph of genus one is achieved when the degree is equal to 2; then 4 transpositions are required. We may use one to attach the subsequent loops, so we need at least 3 transpositions to form the first loop. After that, we may assume that we have two edges of arbitrary ramification which attach one to the previous, the other to the following loop. Again by the Riemann-Hurwitz formula, if both ends have full ramification, then one can make a cycle with two transpositions. But then the two lengths

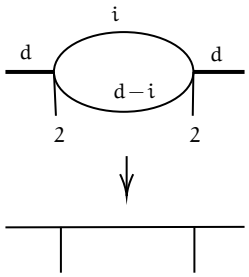

Figure 3.17: A picture of a genus formed using 2 transpositions. The thickened edges show where the previous and next loops would be attached. When $d = 2$ the picture shows the degree 2 loop, in this case only the thickened edge on the right is connected to other loops. The two lengths x, y of the edges of the loop cover the same bounded edge in $\widehat{T}$, therefore they are not independent: they satisfy the relation $ix = (d-i)y$.

of such cycle are not independent, see Figure 3.17. Therefore, each loop needs to cover 2 edges of $\widehat{T}$, and must use at least 3 transpositions. All together $\widehat{\Gamma} \to \widehat{T}$ requires at least $3g$ transpositions. □

Claim 3.2.6. The marked tree part of the graph needs at least g transpositions.

Proof. On the marked tree part of $\Gamma \to T$, there are requirements on the lengths associated with the marked fragments. There are g lengths L_i's, each of which is much longer than any of the lengths on the active path; thus all marked points from 3 to $n-2$ ($g-1$ of them) must be stabilizing to the active path from further down an edge that it is the only mark on. Every time one such edge is formed, at least one transposition must occur. Finally, the branch that the marks $1, 2$ lie on must attach to an edge of degree at least 2, else we would have a relation between the lengths L_1 and x_{4g}. All together, at least g transpositions are needed for the marked tree part of $\Gamma \to T$. □

Since the total number of transpositions is $4g$, the number of transpositions on $\widehat{\Gamma} \to \widehat{T}$ is exactly $3g$ and the number on the rest of $\Gamma \to T$ is g.

Dead ends

We call *dead ends* any part of the graph Γ that gets stabilized away in $\overline{\Gamma}$. Because of the fact that we must be using every transposition to obtain some edge length for either $\overline{\Gamma}$ or $\overline{T}$ dead ends can arise in only two ways: they can be individual ends of degree two, or possibly more complicated subgraphs entirely of degree one.

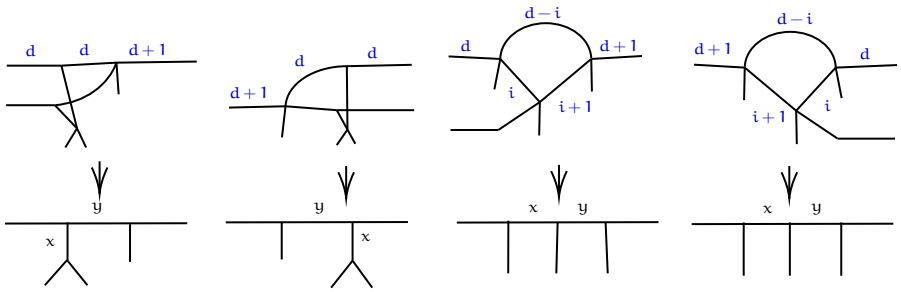

Figure 3.18: The four possible ways to form a genus with 3 transpositions. To avoid cluttering the picture we omit many edges and ends of degree one that would be necessary to draw the complete covers. Also note that the horizontal dead ends are unlabeled because they have degree one.

Genus part

Knowing that any new loop is added with exactly three transpositions, we look at all possible ways to add a new genus to Γ by studying covers of a tree with five ends, two of which may have arbitrary branching data. Due to the graph $\overline{\Gamma}$ needing one much longer edge on each loop, we need to be covering two distinct edges of the base, so no loops formed by pairs of edges between two vertices work. Distinguishing between an incoming and an outgoing end, which connect to the previous loop and the following one, there are four possible covers forming a loop covering two edges, as shown in Figure 3.18. In $\overline{\Gamma}$, we require the 2 lengths of the edges forming each loop to be independent of each other, as one is required to be much longer than the other. Looking at the first picture from the left in Figure 3.18, the loop after stabilization has one edge formed by the horizontal end of degree d, the other by the two diagonal ends of degree one together with the curvy edge of degree one. Let us say that the first edge has length x_t, the second one x_b. With respect to the lengths x, y on the base curve, we have:

$$x_t = \frac{y}{d}, \qquad x_b = 2x + y.$$

One can see that by choosing y much smaller than x one can make the ratio of the two lengths arbitrarily large. The situation is identical for the second picture.

On the other hand, for the third picture let us call x_t the length of the top edge of degree $d-i$ and x_b the length of the edge in the stabilized curved formed by the two edges of degree i and $i+1$. We have

$$x_t = \frac{x+y}{d-i}, \quad x_b = \frac{x}{i} + \frac{y}{i+1}. \tag{3.19}$$

One can see that (3.19) implies that

$$\frac{d-i}{d} x_t \leq x_b \leq (d-i)x_t,$$

showing that the ratio x_b/x_t is bounded both above and below by constants. It is therefore not possible to find an inverse image of the chosen point p that has any loop of this shape. The situation is similar for the fourth picture. In conclusion, every loop must be formed by a fragment of type D, U as described in Section 3.2.2.

Tree part

We now focus our attention on the part of the graph Γ that supports the marked points. We have seen so far that after the last loop there is an active path obtained via a sequence of cuts and joins of the active path with edges of degree one. The marks must stabilize, in reverse order, to each of the trivalent vertices on the active path to obtain $\overline{\Gamma}$. The marked points must lie on inverse images of degree one of some of the fragments F_j described in Section 3.2.2.

Every time a cut occurs, the degree of the active path decreases by 1, and every time a join occurs, the degree of the active path increases by 1. Since joins come from the left and cuts go to the right, in order for both to be covering the same tree of marked points the cut must be to the left of the join. This fact must be true for all cuts and joins covering the first (meaning leftmost) tree in the fragment F_j, therefore all cuts must come before all joins that are covering the first tree. After all of the joins, the graph has as many cuts as needed to decrease the degree of the active path to one. Since the fragments F_j have at most two interesting connected components (interesting here means they are not just a single marked end), the second interesting connected component must be

stabilizing to only cuts - since any join, occurring to the right of the cuts, would leave an active path of degree greater than one.

We conclude that all covers have a marked tree part that looks like some number of cuts followed by all joins and ending with the rest of the cuts. But then all possible solutions to our problem must be of the form of those we have exhibited, and there can be no more solutions. Thus we have concluded the proof of Theorem 3.0.2, and established via a direct tropical computation that $\mathsf{Tev}_g = 2^g$.

Chapter 4

Generalizations of tropical Tevelev degrees

For an integer ℓ, we can generalize the conditions on degree and the number of marked points to let $d = g+1+\ell$ and $n = g+3+2\ell$. These conditions still ensure that the dimension of the moduli space of tropical admissible covers $\mathscr{H}^{\mathtt{trop}}_{g,d,n}$ equals the sum of the dimensions of $\mathscr{M}^{\mathtt{trop}}_{g,n}$ and $\mathscr{M}^{\mathtt{trop}}_{0,n}$. The degree of $(\mathsf{F}_s \times \mathsf{F}_t)$ is the *tropical Tevelev degree* $\mathsf{Tev}^{\mathtt{trop}}_{g,\ell}$.

Computing tropical Tevelev degrees $\mathsf{Tev}^{\mathtt{trop}}_{g,\ell}$ is the same combinatorial inverse problem as we solved in Chapter 3. We start this chapter by considering the case of positive ℓ, where the degree and number of marked points increases for a given genus. This case uses the techniques developed in the previous chapter to prove the following result.

Theorem 4.0.1. *For any positive integers g and ℓ,*

$$\mathsf{Tev}^{\mathtt{trop}}_{g,\ell} = 2^g.$$

The second section of this chapter considers the case of negative ℓ. Navigating this case involves new techniques to count the number of covers that are no longer attainable compared to the $\ell = 0$ base case due to the decrease in the degree. We require that $n \geq 3$ and thus $g+3+2\ell \geq 3$, requiring $g \geq -2\ell$.

Theorem 4.0.2. *For any negative integer ℓ and $g \geq -2\ell$,*

$$\mathsf{Tev}^{\mathtt{trop}}_{g,\ell} = 2^g - \sum_{i=0}^{-\ell-1} \Big(g-2i+1\Big)\left(\binom{g}{i} - \binom{g}{i-1}\right).$$

The correspondence theorem, Theorem 3.0.1, still holds for positive and negative ℓ. The proof remains unchanged. Due to this, we have provided tropical proofs of Tevelev degree computations done in [11]. These proofs first provide a combinatorial understanding of why increasing to a positive ℓ does not change the count of 2^g. This is because we build the grid of solutions using

the same genus sections of the covers and connect them to the marked point sections of the covers from the genus $g+2\ell$ covers from the $\ell=0$ case. The second proof provides a combinatorial understanding of the defect from 2^g. We are subtracting away sections of the grid where $\binom{g}{i}-\binom{g}{i-1}$ corresponds to how many rows we are removing and $g-2i+1$ is how many columns wide that group of rows is.

4.1 $\ell > 0$ case

When ℓ becomes positive, the degree and number of marked points both increase. When comparing to the $\ell=0$ case, the degree becomes ℓ larger and there is 2ℓ more marked points for a given genus. When constructing the covers $\Gamma \to T$ for positive ℓ, we end up with the same genus part of the cover $\widehat{\Gamma} \to \widehat{T}$ as the $\ell=0$ case. From here we add on the marked fragments from the $g+2\ell$ covers of the $\ell=0$ case. Piecing together these different pieces from the $\ell=0$ case ends up giving us the same total count of 2^g. We now go over some examples in low genera and low ℓ to demonstrate these ideas and then prove the total count.

4.1.1 Examples in low genera and low ℓ

$\ell=1$:

Starting with $g=1$, in order to compute $\mathsf{Tev}_{1,1}^{\mathtt{trop}}$, we must compute the degree of the map

$$(\mathsf{F_s}\times\mathsf{F_t}):\mathscr{H}_{1,3,6}^{\mathtt{trop}}\to\mathscr{M}_{1,6}^{\mathtt{trop}}\times\mathscr{M}_{0,6}^{\mathtt{trop}}.$$

Consider the point $p=(\overline{\Gamma},\overline{T})\in\mathscr{M}_{1,6}^{\mathtt{trop}}\times\mathscr{M}_{0,6}^{\mathtt{trop}}$ depicted in Figure 4.1. The set $(\mathsf{F_s}\times\mathsf{F_t})^{-1}(p)$ consists of covers $\phi:\Gamma\to T$ such that T stabilizes to $\overline{T}$ when forgetting the six marked ends with branching data (2), and Γ stabilizes to $\overline{\Gamma}$ when forgetting the six marked ends with expansion factor 2 as well as all the unmarked ends.

We start constructing Γ and T by creating the genus zero part, containing the marked points. Due to the cover being degree 3, there will be one edge cutting from the active edge to end with a

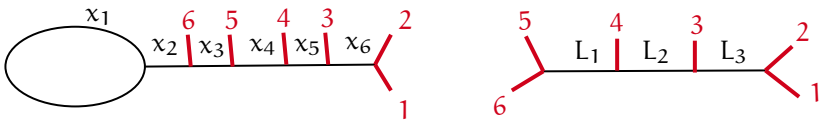

Figure 4.1: The point p in $\mathscr{M}_{1,6}^{\mathtt{trop}} \times \mathscr{M}_{0,6}^{\mathtt{trop}}$. We have $x_1 << x_2 << x_3 << x_4 << x_5 << x_6 << L_1 << L_2 << L_3$.

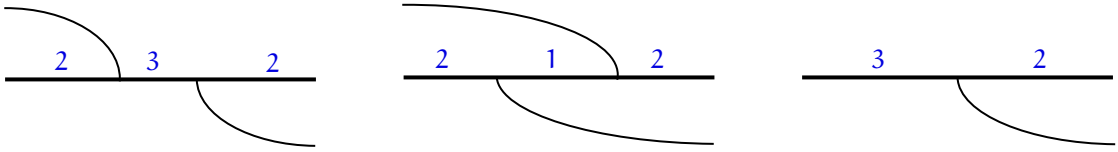

Figure 4.2: The three options for a genus zero graph containing one cut and at most one join.

transposition and at most one edge joining the active edge, because the genus could be degree 2 or 3. Therefore, we have three options for the genus zero part of Γ, shown in figure 4.2.

When placing marked points on the options for Γ, there are three L_i's, therefore three lengths need to be free to be made long. The marked point fragments shown in 4.3 each have 3 vertical lengths that when placed correctly on a cover, will allow for the three L_i's to be made long. The fragment on the left hand side requires a cover with 3 edges on the left hand side covering the tree with three marked points and it needs 2 edges covering the tree on the right hand side. Therefore, the fragment on the left side of figure 4.3 can be placed on the genus zero graph in the middle of figure 4.2. Similarly, the fragment on the right hand side of figure 4.3 can only be placed on the graph on the left of figure 4.2.

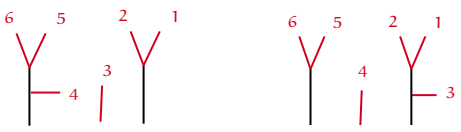

Figure 4.3: Two configurations of marked points that allow for three long edges to be forgotten in the stabilization of the cover curve.

The genus zero part of the $\Gamma \to Ts$ that we are constructing both use three transpositions, therefore we have 3 transpositions left to create $\widehat{\Gamma} \to \widehat{T}$. There is a unique way to form a loop with 3 transpositions. Putting this loop together with the genus zero parts discussed above, we can now place the marked fragments on Γ and T.

For one cover, start with a simple loop using three transpositions, then have an edge cut from the active edge at a distance of y_2 away from the loop. Next, have an edge join the active edge at a distance of $y_3 + y_4$ to the right of the cutting edge. Looking at T_1, place a tree with three marked points to the right y_3 from the fourth transposition. There are three trees in Γ_1 covering this tree in T_1. Place the marked point 6 at the end of the tree on the edge cutting from the active edge covering T_1, then place the marked point 5 at the end of the tree on the active edge. On the tree lying on the edge joining the active edge, place the marked point 4 at the distance y_6 down from 5 and 6. Moving to the right, place the marked point 3 y_7 away from the edge joining, then y_8 to the right, place the marked points 1 and 2 on separate trees of length y_9.

Place the points in a similar way for $\Gamma_2 \to T_2$, but with the cut and join switched. Together, we have the two covers shown in figure 4.4.

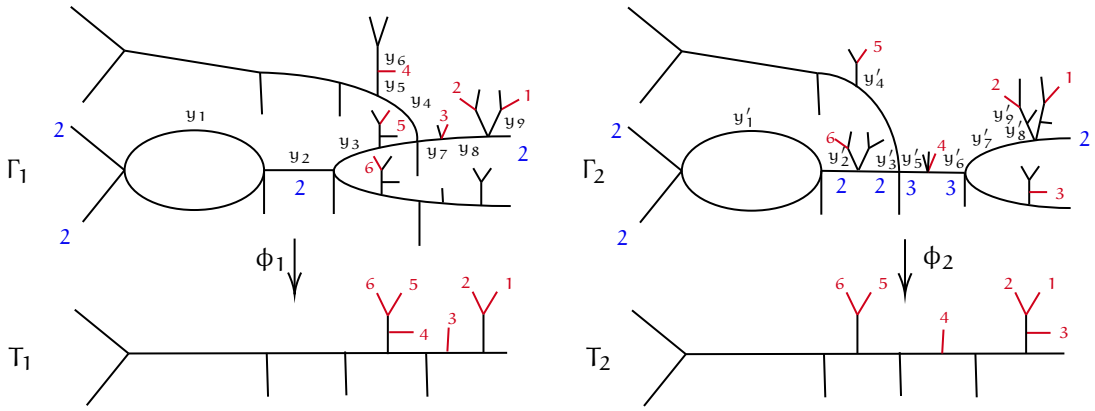

Figure 4.4: The two covers in $((F_s \times F_t))^{-1}(p)$ for $\ell = 1$ and $g = 1$.

We now compute the local degree of $(F_s \times F_t)$ at these inverse images, which gives us the multiplicities which we need to count the covers. The multiplicity of the inverse image is the

product of three factors: an automorphism factor, a product of local Hurwitz numbers and a dilation factor corresponding to the determinant of the matrix representing the map $F_s \times F_t$.

To calculate the local Hurwitz numbers for cover 1, every vertex in Γ_1 is either trivalent with degree one edges in all directions or two edges of degree 2 in different directions and 2 edges of degree 1 in the same direction. Both of these types of vertices have local Hurwitz number equal to 1, therefore the product of all local Hurwitz numbers is 1. Additionally, Γ_2 contains vertices with an edge of degree 3 in one direction and simple transpositions in the other 2 directions, as well as a vertex with two directions containing an edge of degree 3 and three edges of degree 1 in the third direction. The first of these vertex options has local Hurwitz number equal to 1. The second option, we are marking one of the edges of degree 1, so the local Hurwitz number is also equal to 1. All together, the product of local Hurwitz numbers is equal to 1.

For each cover, we have one factor of 2 corresponding to switching simultaneously the two unlabeled left ends of branching type 2 and their inverse images. Also, a second factor of 2 consists of switching the two degree 1 edges of Γ_i forming the loop. However, this is also a nontrivial automorphism of $\overline{\Gamma_i}$. Altogether, we have

$$\frac{|\mathrm{Aut}(\overline{\Gamma_i})|}{|\mathrm{Aut}(\phi_i)|} = \frac{1}{2}. \tag{4.1}$$

To calculate the dilation factors, we set up the following matrices representing the x_i's and L_j's in terms of the y_k's:

$$M_1 = \begin{array}{c} \\ x_1 \\ x_2 \\ x_3 \\ x_4 \\ x_5 \\ x_6 \\ L_1 \\ L_2 \\ L_3 \end{array} \begin{array}{c} \begin{array}{ccccccccc} y_1 & y_2 & y_3 & y_4 & y_5 & y_6 & y_7 & y_8 & y_9 \end{array} \\ \begin{bmatrix} 2 & 0 & 0 & 0 & 0 & 0 & 0 & 0 & 0 \\ 0 & 1 & 0 & 0 & 0 & 0 & 0 & 0 & 0 \\ 0 & 0 & 1 & 0 & 0 & 0 & 0 & 0 & 0 \\ 0 & 0 & 0 & 1 & 0 & 0 & 0 & 0 & 0 \\ 0 & 0 & 0 & 0 & 0 & 0 & 1 & 0 & 0 \\ 0 & 0 & 0 & 0 & 0 & 0 & 0 & 1 & 0 \\ 0 & 0 & 0 & 0 & 0 & 1 & 0 & 0 & 0 \\ 0 & 0 & 0 & 1 & 1 & 0 & 2 & 0 & 0 \\ 0 & 0 & 0 & 0 & 0 & 0 & 0 & 2 & 1 \end{bmatrix} \end{array} \qquad M_2 = \begin{array}{c} \\ x_1 \\ x_2 \\ x_3 \\ x_4 \\ x_5 \\ x_6 \\ L_1 \\ L_2 \\ L_3 \end{array} \begin{array}{c} \begin{array}{ccccccccc} y_1' & y_2' & y_3' & y_4' & y_5' & y_6' & y_7' & y_8' & y_9' \end{array} \\ \begin{bmatrix} 2 & 0 & 0 & 0 & 0 & 0 & 0 & 0 & 0 \\ 0 & 1 & 0 & 0 & 0 & 0 & 0 & 0 & 0 \\ 0 & 0 & 1 & 0 & 0 & 0 & 0 & 0 & 0 \\ 0 & 0 & 0 & 0 & 1 & 0 & 0 & 0 & 0 \\ 0 & 0 & 0 & 0 & 0 & 1 & 0 & 0 & 0 \\ 0 & 0 & 0 & 0 & 0 & 0 & 1 & 0 & 0 \\ 0 & 0 & 2 & 1 & 3 & 0 & 0 & 0 & 0 \\ 0 & 0 & 0 & 0 & 0 & 3 & 2 & 1 & 0 \\ 0 & 0 & 0 & 0 & 0 & 0 & 0 & 0 & 1 \end{bmatrix} \end{array}$$

We see that $|\det M_i| = 2$ for $i = 1, 2$. All together the multiplicity of each cover in $(F_s \times F_t)^{-1}(p)$ is $1 \cdot \frac{1}{2} \cdot 2 = 1$. Since we have two inverse images each with multiplicity one, we obtain $\mathsf{Tev}_{1,1}^{\mathtt{trop}} = 2$.

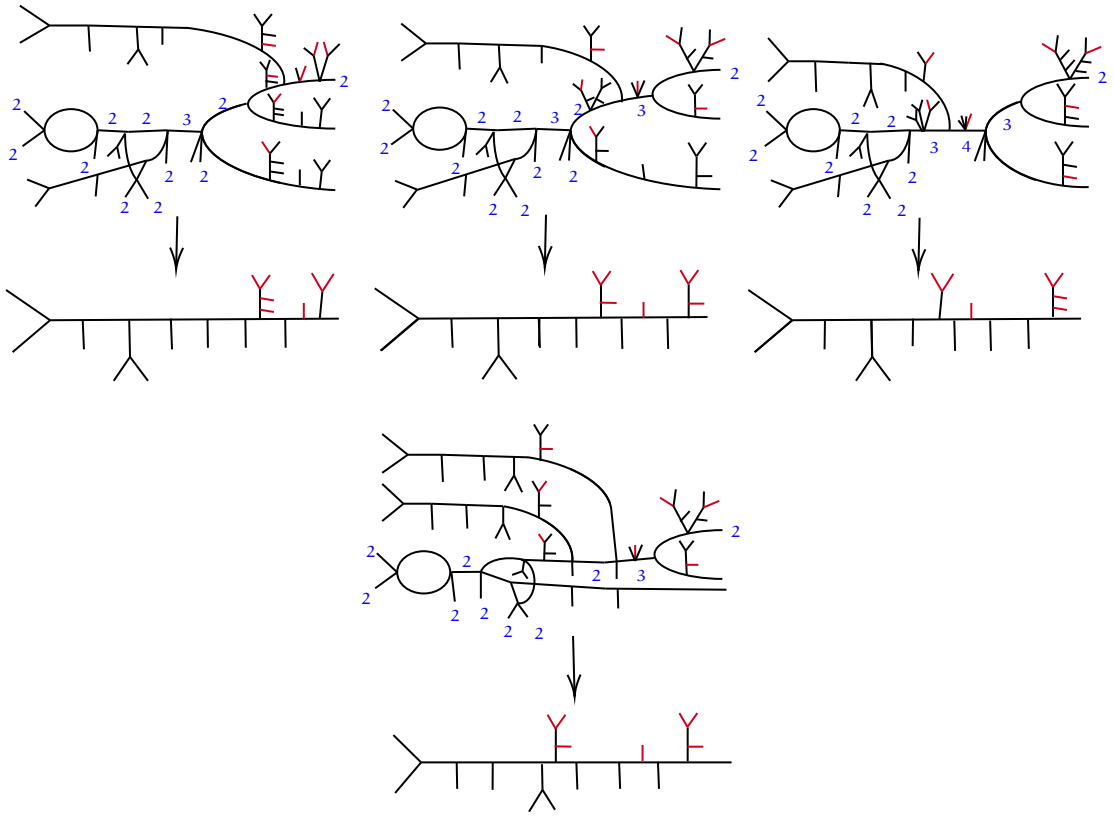

Figure 4.5: The four covers in $((F_s \times F_t))^{-1}(p)$ for $\ell = 1$ and $g = 2$.

Next, looking at $g = 2$, there are 4 preimages as shown in figure 4.5, each with multiplicity 1, so $\mathsf{Tev}_{2,1}^{\mathtt{trop}} = 4$

$\ell = 2$**:**

To compute $\mathsf{Tev}_{1,2}^{\mathtt{trop}}$, we look for the degree of the map

$$F_s \times F_t : \mathscr{H}_{1,4,8}^{\mathtt{trop}} \to \mathscr{M}_{1,8}^{\mathtt{trop}} \times \mathscr{M}_{0,8}^{\mathtt{trop}}. \tag{4.2}$$

We consider the point $p = (\overline{\Gamma}, \overline{T}) \in \mathscr{M}_{1,8}^{\mathtt{trop}} \times \mathscr{M}_{0,8}^{\mathtt{trop}}$ built according to the general form shown in Figure 4.6. There are 2 preimages as shown in Figure 4.7, each with multiplicity 1, so $\mathsf{Tev}_{1,2}^{\mathtt{trop}} = 2$. Note that the genus is formed in 3 simple transpositions, exactly as in the $\ell = 0$ and 1 cases.

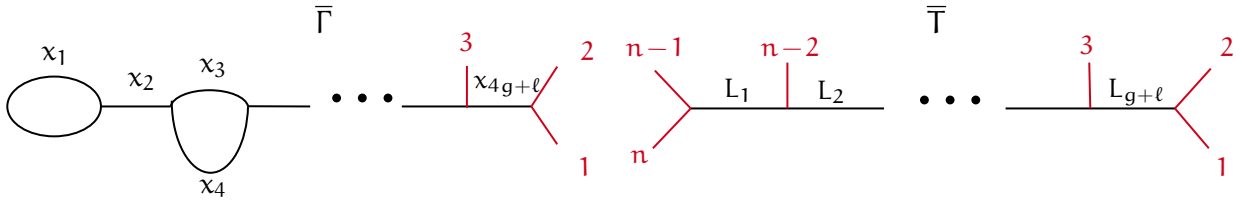

Figure 4.6: The graphs $\overline{\Gamma}, \overline{T}$ defining the chosen point p of $\mathscr{M}_{g,n}^{\mathtt{trop}} \times \mathscr{M}_{0,n}^{\mathtt{trop}}$.

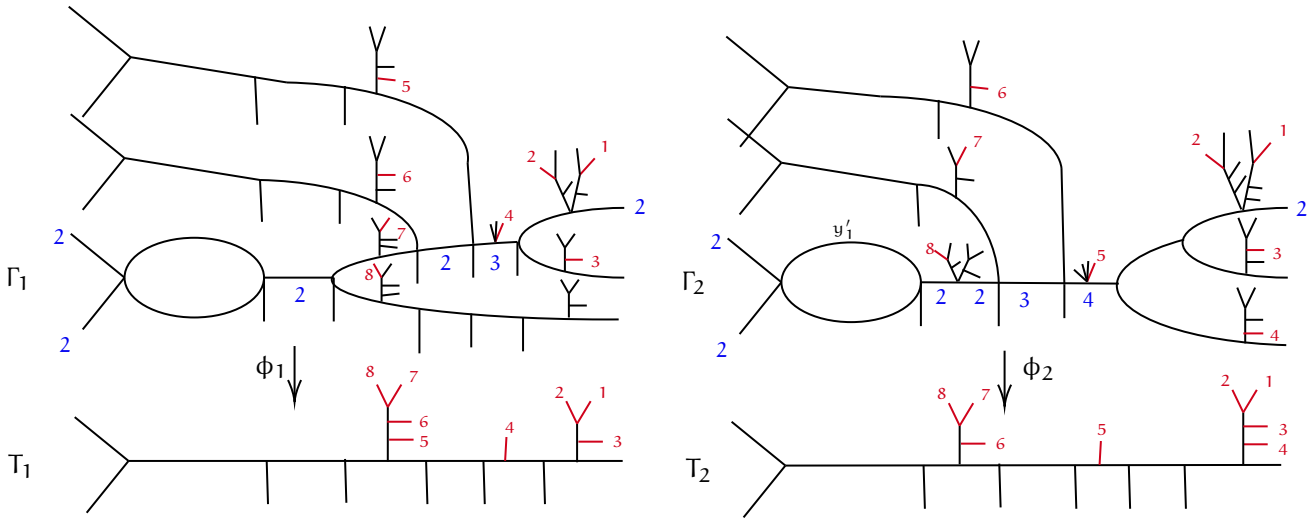

Figure 4.7: The two covers in $((F_s \times F_t))^{-1}(p)$ for $\ell = 2$ and $g = 1$.

4.1.2 Construction of 2^g solutions

In this section we make explicit and generalize the constructions from the examples in the previous section and construct 2^g preimages of p for any genus g. We build covers containing all the genus, construct trees containing the n marked ends, and show that the multiplicity of every cover constructed is equal to 1.

The genus part

We construct the genus part in the same way as in Section 3.2.2. Recall that every cover starts with a degree 2 loop using 3 simple transpositions, and a fourth simple transposition leading into the active edge. For $g > 1$, we then add one of two genus options, U and D as shown in Figure 3.9,

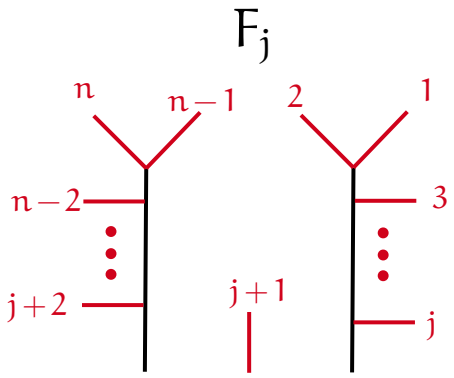

Figure 4.8: The marked fragment that attaches to the horizontal edge of $\tilde{T}$ to obtain the base graph T.

for each loop. Note that U can always be added, while D can only be added if the degree of the active edge is greater than 2. If the fragment D has been used i times, we obtain a connected cover of degree $g+1-i$. We complete it to a degree $g+1+\ell$ cover by adding $i+\ell$ disjoint copies of the base curve, each mapping of degree one. Call these disjoint copies of the base curve that are added, *joined ends*.

The marked tree part

We construct the marked tree part by taking the fragment F_j shown in Figure 4.8 when $3+\ell \leq j \leq n-\ell$. These markings are placed on the tree in the same way as in Section 3.2.2. Since we are constructing the covers from the same pieces as we did in Section 3.2.2, no work is needed to show the multiplicity of every cover constructed equals 1.

The number of marked fragments when $\ell > 0$ is $n-2-2\ell = g+3+2\ell-2-2\ell = g-1$. There is a bijection between this solution set and the solution set constructed in Section 3.2.2. Since each cover counts with multiplicity equal to one, we have thus far shown that $\mathsf{Tev}^{\mathtt{trop}}_{g,\ell} \geq 2^g$ for positive ℓ.

4.1.3 Excluding further solutions

In this section, we exclude any further cover $\Gamma \to T$ from mapping to the chosen point $p = (\overline{\Gamma}, \overline{T}) \in \mathscr{M}^{\mathtt{trop}}_{g,n} \times \mathscr{M}^{\mathtt{trop}}_{0,n}$. We follow similar arguments made in Section 3.2.3.

Fragments attaching to the active edge

The same argument as in Section 3.2.3 excludes all marked fragments besides those shown in Figure 3.12. We now exclude marked fragments F_1 and F_{n-2}.

Section 3.2.2 explains that marked fragments F_1 and F_{n-2} can only be placed on covers that have $i = 0$, meaning that zero joined ends have to be added to complete the degree $d = g+1$ cover. When ℓ is positive, we must add ℓ joined ends to obtain a cover of degree $d+g+1+\ell$. Therefore, even when fragment D is used zero times, $i > 0$. Moreover, only the marked fragments shown in Figure 4.8 can be attached to covers.

Splitting of transpositions

Recall that the genus part of the graph $\widehat{\Gamma} \to \widehat{T}$ contains at least $3g$ transpositions.

Claim 4.1.1. The marked tree part of the graph needs at least $g+2\ell$ transpositions.

Proof. There are $g+2\ell$ lengths L_i's, each of which is much longer than the lengths on $\overline{\Gamma}$. Therefore, all marked points from 3 to $n-2 = g+1+2\ell$ must be stabilizing to the active path from an edge that it is the only mark on. There are at least $g+2\ell-1$ transpositions used to form such edges. Finally, in order to not have a relation between the lengths $x_{4g+2\ell}$ and $L_{g+2\ell}$, the branch that the marks 1 and 2 lie on must attach to an edge of degree at least 2. In total, at least $g+2\ell$ transpositions are needed for the marked tree part of $\Gamma \to T$. □

The total number of transpositions is $4g+2\ell$, and therefore the number of transpositions on $\widehat{\Gamma} \to \widehat{T}$ is exactly $3g$ and the number on the marked tree part of $\Gamma \to T$ is $g+2\ell$.

Knowing that any new loop is added with exactly three transpositions we use the proof in Section 3.2.3 to rule out all loop fragments besides U and D. Section 3.2.3 also gives that all covers have a marked tree part that looks like some number of cuts followed by all joins and ending with the rest of the cuts. But then all possible solutions to our problem must be of the form of those we have exhibited, and there can be no more solutions and we have shown Theorem 4.0.1.

4.2 $\ell < 0$ case

When ℓ is negative, both the degree and the number of marked points become less than what they are in the $\ell = 0$ case. Due to the degree being lower, we can not form the genus section of the covers in all of the same ways. If a genus part of the cover, $\widehat{\Gamma} \to \widehat{T}$, from the $\ell = 0$ case used all of the degree to form the genus, that can not be made when the degree decreases. This leads to fewer ways to form the genus section. We can count the number of preimages using the same grid as used in the $\ell = 0$ case but there are rows removed corresponding to the $\widehat{\Gamma} \to \widehat{T}$ from the $\ell = 0$ case that are not possible. In this section, we go through examples in low genera when $\ell = -1$, then construct the number of solutions, and finally rule out any other possible solutions.

4.2.1 Examples in low genera and high ℓ

$\ell = -1$**:**

Starting with $g = 2$, in order to compute $\mathsf{Tev}^{\mathtt{trop}}_{2,-1}$, we must compute the degree of the map

$$(\mathsf{F_s} \times \mathsf{F_t}) : \mathscr{H}^{\mathtt{trop}}_{2,2,3} \to \mathscr{M}^{\mathtt{trop}}_{2,3} \times \mathscr{M}^{\mathtt{trop}}_{0,3}.$$

Consider the point $p = (\overline{\Gamma}, \overline{T}) \in \mathscr{M}^{\mathtt{trop}}_{2,3} \times \mathscr{M}^{\mathtt{trop}}_{0,3}$ depicted in Figure 4.6.

We start by constructing $\widehat{\Gamma} \to \widehat{T}$. The Riemann-Hurwitz formula states that there are 6 simple transpositions. There is one way to form a degree 2 cover that contains two disjoint loops.

We then complete $\widehat{\Gamma} \to \widehat{T}$ to $\Gamma \to T$ by adding 3 marked points. Place marked point 3 at distance y_5 from the second loop, and place marked points 1 and 2 y_6 to the right on 3. There are no other ways to place the marked points so that $\Gamma \to T$ is a preimage of p. Therefore, we get one cover in $(\mathsf{F_s} \times \mathsf{F_t})^{-1}(p)$ shown in Figure 4.9. We now compute the local degree of $(\mathsf{F_s} \times \mathsf{F_t})$ at this inverse image.

To calculate the local Hurwitz number, every vertex in Γ_1 is either trivalent with degree one edges in all directions or two edges of degree 2 in different directions and 2 edges of degree 1 in the

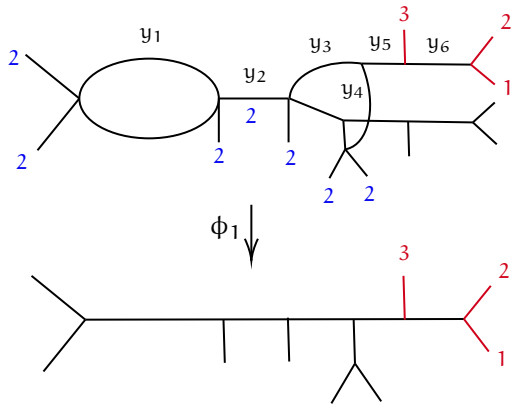

Figure 4.9: The one cover in $(F_s \times F_t)^{-1}(p)$ for $\ell = -1$ and $g = 2$.

same direction. Both of these types of vertices have local Hurwitz number equal to 1, therefore the product of all local Hurwitz numbers is 1.

The cover has an automorphism factor of 2 corresponding to switching each pair of ends of branching type 2 and their inverse images. Altogether, we have

$$\frac{|\mathrm{Aut}(\overline{\Gamma_1})|}{|\mathrm{Aut}(\phi_1)|} = \frac{1}{4}.$$

To calculate the dilation factor, we set up the following matrix representing the x_i's in terms of the y_k's:

$$M_1 = \begin{array}{c} \\ x_1 \\ x_2 \\ x_3 \\ x_4 \\ x_5 \\ x_6 \end{array} \begin{array}{c} \begin{array}{cccccc} y_1 & y_2 & y_3 & y_4 & y_5 & y_6 \end{array} \\ \begin{bmatrix} 2 & 0 & 0 & 0 & 0 & 0 \\ 0 & 1 & 0 & 0 & 0 & 0 \\ 0 & 0 & 1 & 0 & 0 & 0 \\ 0 & 0 & 1 & 2 & 0 & 0 \\ 0 & 0 & 0 & 0 & 1 & 0 \\ 0 & 0 & 0 & 0 & 0 & 1 \end{bmatrix} \end{array}$$

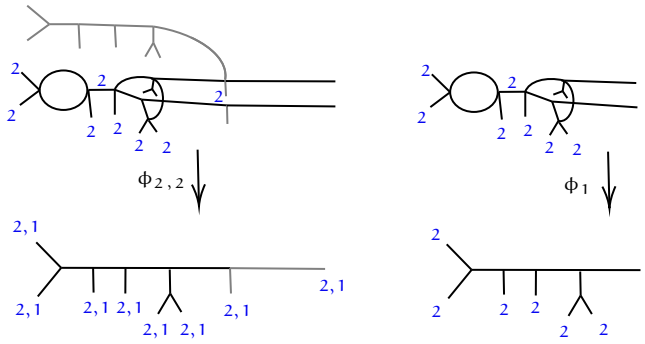

Figure 4.10: The cover $\phi_{2,2}$ with the joined end removed and no marked points is the same as ϕ_1 in with no marked points.

We see that $|\det M_1| = 4$. All together the multiplicity of each cover in $(\mathsf{F_s} \times \mathsf{F_t})^{-1}(p)$ is $1 \cdot \frac{1}{4} \cdot 4 = 1$. Since we have one inverse image with multiplicity one, we obtain $\mathsf{Tev}^{\mathtt{trop}}_{2,-1} = 1$.

To interpret $\mathsf{Tev}^{\mathtt{trop}}_{2,-1}$ in another way, we compare the grid of solutions for $\ell = -1$ and $g = 2$ with the grid of solutions for $\ell = 0$ and $g = 2$ shown in Figure 3.6. Although the marked point configurations and total degrees are different, we obtain organizations according to the same active edge degrees. When $\ell = -1$, we lose the top row of the grid corresponding to having an active edge of degree 3. The cover $\phi_{2,2}$ in Figure 3.6 with the joined end removed and no marked points is the same as ϕ_1 in Figure 4.9 with no marked points as shown in Figure 4.10.

Moving to genus 3, to compute $\mathsf{Tev}^{\mathtt{trop}}_{3,-1}$, we must compute the degree of the map

$$(\mathsf{F_s} \times \mathsf{F_t}) : \mathscr{H}^{\mathtt{trop}}_{3,3,4} \to \mathscr{M}^{\mathtt{trop}}_{3,4} \times \mathscr{M}^{\mathtt{trop}}_{0,4}.$$

We start by constructing $\widehat{\Gamma} \to \widehat{\mathsf{T}}$. Looking at Figure 4.11, for $g = 3$, there are 3 possible paths, but one of those paths ends at a vertex with active edge degree 4. Since $\ell = -1$, the degree of the cover is 3, therefore, paths to that vertex are not possible. We conclude that there are two possible ways to construct $\widehat{\Gamma} \to \widehat{\mathsf{T}}$, one by adding U then D and one by doing the opposite. Recall U and D are introduced in Figure 3.9. Note, both of these options have an active edge of degree 2.

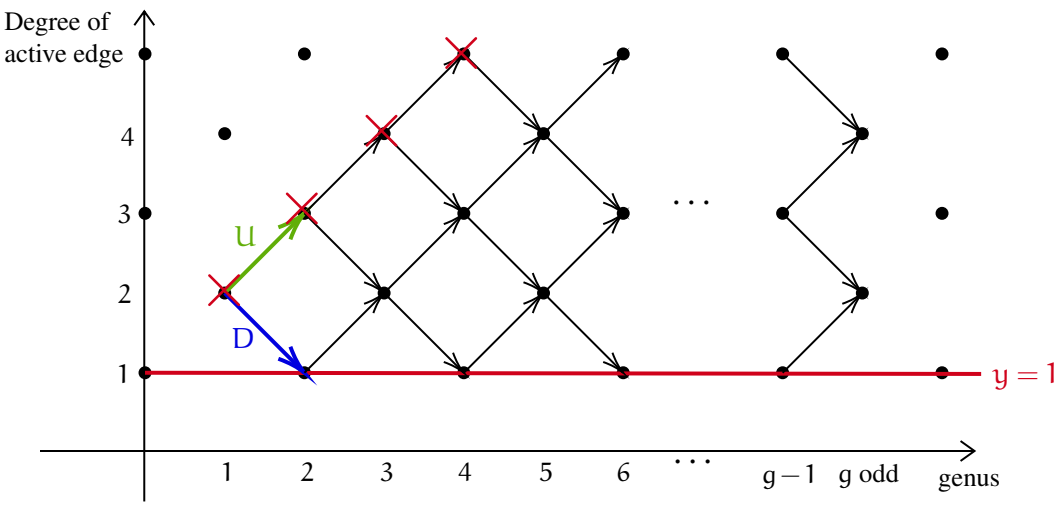

Figure 4.11: A graph showing for genus g which degrees are possible for the active edge by adding U and D. For $\ell = -1$, paths ending at vertices along the diagonal are not possible because $d = g$.

To complete the cover, we add 4 marked points. The task of adding 4 marked points to an active edge of degree 2 was done in detail in Chapter 3.2.1, there are 2 ways of doing so. Putting together the ways to form $\widehat{\Gamma} \to \widehat{T}$ with the ways to add marked points, we have 4 total covers in the preimage of p, giving that $\mathsf{Tev}^{\mathrm{trop}}_{3,-1} = 4$. Comparing the genus 3 grid of solutions when $\ell = -1$ in Figure 4.12 to the grid of solutions when $\ell = 0$ shown in Figure 3.8, notice that the prior is missing the top row of solutions.

4.2.2 Construction of solutions

$\ell = -1$**:**

We start constructing the number of solutions for general g for the case when $\ell = -1$. We construct the genus part in a similar fashion to the construction in Chapter 3.2.2, but there are fewer options for any given genus g due to the condition that $d = g + 1 + \ell$. When $\ell = -1$, $d = g$, which restricts paths from ending at vertices on the diagonal, i.e. there is at least one D added, as shown in Figure 4.11. In terms of the grid of solutions we built in the $\ell = 0$ case, we lose the rows of solutions corresponding to an active edge of degree $g + 1$. This number of rows is equal to the number of paths ending at a vertex on the diagonal, which is equal to $\binom{g}{0} = 1$.

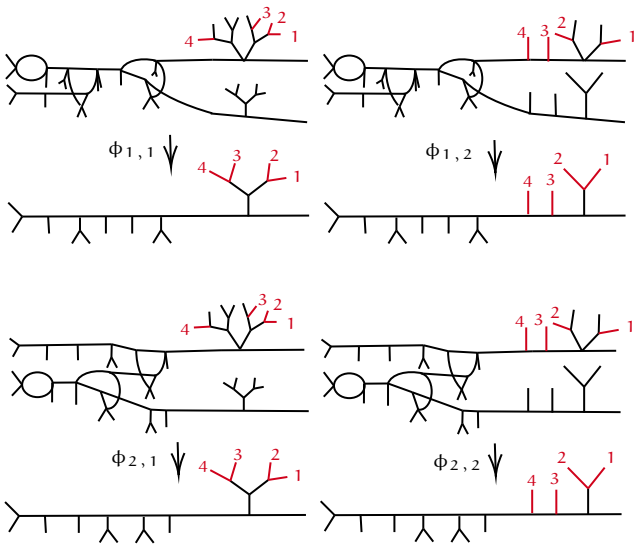

Figure 4.12: The four covers in $(F_s \times F_t)^{-1}(p)$ when $\ell = -1$ and $g = 3$.

The number of marked points $n = g+3-2 = g+1$, is the same number of marked points as in the $\ell = 0$ case when the genus is 2 less. The marked fragments presented in Section 3.2.2 for n marked points can be placed on the same active edge degrees as we have remaining in our grid of solutions.

Altogether, solutions can be thought of as the number of solutions when $\ell = 0$ minus the solutions corresponding to an active edge of degree $g+1$. The number of columns that are filled in these rows is equal to the number of marked fragments, $g+1$. The total number of solutions constructed is equal to $2^g - (g+1)\binom{g}{0}$.

$\ell < 0$: The genus part

We again construct the genus part in a similar fashion to the construction in Chapter 3.2.2, but there are fewer options for any given genus g. When $\ell = -i$, $d = g+1-i$, there must be at least i D's added, giving an active edge of degree less than or equal to $g+1-2i$ in addition to i free ends coming from each of the i D's added. Therefore, ℓ being negative does not allow paths to end at vertices less than or equal to ℓ steps down from the diagonal. In terms of the grid of solutions, we lose the rows of solutions corresponding to active edge degrees greater than $g+1-2i$. The number

of rows of the grid that come from a given active edge degree is equal to the number of paths to the corresponding vertex, which is equal to $(\binom{g}{i} - \binom{g}{i-1})$ for active edge degree $g+1-2i$.

The marked tree part

For genus g, there are $n-2 = g+1+2\ell$ fragments coming from the $g+2\ell$ case of the $\ell = 0$ case. These are placed on the marked part of the cover in the same way as described in 3.2.2. Since we are constructing the covers from the same pieces as we did in Section 3.2.2, no work is needed to show the multiplicity of every cover constructed equals 1.

When $\ell = 0$, we have shown that every type of fragment can be placed on the cover with the highest possible active degree, therefore not having those covers, takes away $(g+1)\binom{g}{0}$ covers from 2^g. For every vertex down that corresponds to unattainable paths, there are two fewer marked fragments that can be placed. Each vertex corresponds to $(g+1-2i)(\binom{g}{i} - \binom{g}{i-1})$ covers where i is the number of vertices down because there are $(g+1-2i)$ marked fragment options and $(\binom{g}{i} - \binom{g}{i-1})$ genus part options.

For positive integer g and negative integer ℓ,

$$\mathsf{Tev}_{g,\ell}^{\mathtt{trop}} \geq 2^g - \sum_{i=0}^{-\ell-1} \left(g-2i+1\right)\left(\binom{g}{i} - \binom{g}{i-1}\right).$$

4.2.3 Excluding further solutions

In this section, we exclude any further cover $\Gamma \to T$ from mapping to the chosen point $p = (\overline{\Gamma}, \overline{T}) \in \mathscr{M}_{g,n}^{\mathtt{trop}} \times \mathscr{M}_{0,n}^{\mathtt{trop}}$. We follow similar arguments made in Section 3.2.3.

For ℓ negative, there are $n = g+3+2\ell$ markings. This is the same number of marked points as the $g+2\ell$ case of $\ell = 0$. These marked points can be placed in marked fragments as shown in Figure 3.12. The same argument as in Section 3.2.3 excludes all other marked fragments.

Recall from Section 4.1.3 that the total number of transpositions is $4g+2\ell$, and therefore the number of transpositions on $\widehat{\Gamma} \to \widehat{T}$ is exactly $3g$ and the number on the marked tree part of $\Gamma \to T$ is $g+2\ell$.

Knowing that any new loop is added with exactly three transpositions we use the proof in Section 3.2.3 to rule out all loop fragments besides U and D. Section 3.2.3 also gives that all joins happen in a row. Then all possible solutions to our problem must be of the form of those we have exhibited, and there can be no more solutions and thus we have shown Theorem 4.0.2.

Bibliography

[1] Jenia Tevelev. Scattering amplitudes of stable curves. Preprint:arXiv:2007.03831, 2020.

[2] Anders Buch and Rahul Pandharipande. Tevelev degrees in Gromov-Witten theory. Preprint:arXiv:2112.14824, 2021.

[3] Alessio Cela and Carl Lian. Fixed-domain curve counts for blow-ups of projective space. Preprint:arXiv:230303433, 2023.

[4] Carl Lian. Degenerations of complete collineations and geometric Tevelev degrees of $\mathbb{P}^r$. Preprint:arXiv:2308.00046, 2023.

[5] Alessio Cela and Aitor Iribar Lopez. Genus 0 logarithmic and tropical fixed-domain counts for Hirzebruch surfaces. *J. Lond. Math. Soc. (2)*, 109(4):Paper No. e12892, 28, 2024.

[6] Kenneth Intriligator. Fusion residues. *Modern Phys. Lett. A*, 6(38):3543–3556, 1991.

[7] Aaron Bertram. Towards a Schubert calculus for maps from a Riemann surface to a Grassmannian. *Internat. J. Math.*, 5(6):811–825, 1994.

[8] Aaron Bertram, Georgios Daskalopoulos, and Richard Wentworth. Gromov invariants for holomorphic maps from Riemann surfaces to Grassmannians. *J. Amer. Math. Soc.*, 9(2):529–571, 1996.

[9] Bernd Siebert and Gang Tian. On quantum cohomology rings of Fano manifolds and a formula of Vafa and Intriligator. *Asian J. Math.*, 1(4):679–695, 1997.

[10] Alina Marian and Dragos Oprea. Virtual intersections on the Quot scheme and Vafa-Intriligator formulas. *Duke Math. J.*, 136(1):81–113, 2007.

[11] A. Cela, R. Pandharipande, and J. Schmitt. Tevelev degrees and Hurwitz moduli spaces. *Math. Proc. Cambridge Philos. Soc.*, 173(3):479–510, 2022.

[12] Alessio Cela and Carl Lian. Generalized Tevelev degrees of $\mathbb{P}^1$. *J. Pure Appl. Algebra*, 227(7):Paper No. 107324, 30, 2023.

[13] Renzo Cavalieri, Hannah Markwig, and Dhruv Ranganathan. *Tropical and logarithmic methods in enumerative geometry*, volume 52 of *Oberwolfach Seminars*. Birkhäuser/Springer, Cham, [2023] ©2023.

[14] Renzo Cavalieri and Erin Dawson. Tropical tevelev degrees, 2024.

[15] Hannah Markwig. Tropical curves and covers and their moduli spaces. *Jahresber. Dtsch. Math.-Ver.*, 122(3):139–166, 2020.

[16] Renzo Cavalieri and Eric Miles. Riemann surfaces and algebraic curves: A first course in hurwitz theory. 2016.

[17] Renzo Cavalieri, Paul Johnson, and Hannah Markwig. Tropical hurwitz numbers, 2010.

[18] Joachim Kock and Israel Vainsencher. *An invitation to quantum cohomology*, volume 249 of *Progress in Mathematics*. Birkhäuser Boston, Inc., Boston, MA, 2007. Kontsevich's formula for rational plane curves.

[19] Joe Harris and Ian Morrison. *Moduli of curves*, volume 187 of *Graduate Texts in Mathematics*. Springer-Verlag, New York, 1998.

[20] Joe Harris and David Mumford. On the Kodaira dimension of the moduli space of curves. *Invent. Math.*, 67(1):23–88, 1982. With an appendix by William Fulton.

[21] Grigory Mikhalkin. Moduli spaces of rational tropical curves. In *Proceedings of Gökova Geometry-Topology Conference 2006*, pages 39–51. Gökova Geometry/Topology Conference (GGT), Gökova, 2007.

[22] Dan Abramovich, Lucia Caporaso, and Sam Payne. The tropicalization of the moduli space of curves. *Ann. Sci. Ec. Norm. Super.*, 48(4):765–809, 2015.

[23] Lucia Caporaso. Gonality of algebraic curves and graphs. In *Algebraic and complex geometry*, volume 71 of *Springer Proc. Math. Stat.*, pages 77–108. Springer, Cham, 2014.

[24] Renzo Cavalieri, Hannah Markwig, and Dhruv Ranganathan. Tropicalizing the space of admissible covers. *Math. Ann.*, 364(3-4):1275–1313, 2016.

[25] Grigory Mikhalkin. Tropical geometry and its applications. In *International Congress of Mathematicians*, volume 2, page 827–852. Eur. Math. Soc., Zürich, 2006.

[26] Lars Allermann and Johannes Rau. First steps in tropical intersection theory. *Mathematische Zeitschrift*, 264(3):633–670, 2010.

[27] Eric Katz. Tropical intersection theory from toric varieties. *Collect. Math.*, 63(1):29–44, 2012.

[28] Kristin Shaw. A tropical intersection product in matroidal fans. *SIAM J. Discrete Math.*, 27(1):459–491, 2013.

[29] Andreas Gross. Intersection theory on tropicalizations of toroidal embeddings. *Proc. Lond. Math. Soc. (3)*, 116(6):1365–1405, 2018.

[30] Andreas Gathmann, Michael Kerber, and Hannah Markwig. Tropical fans and the moduli spaces of tropical curves. *Compos. Math.*, 145(1):173–195, 2009.

[31] Diane Maclagan and Bernd Sturmfels. *Introduction to tropical geometry*, volume 161 of *Graduate Studies in Mathematics*. American Mathematical Society, Providence, RI, 2015.

[32] Renzo Cavalieri, Andreas Gross, and Hannah Markwig. Tropical ψ classes. *Geom. Topol.*, 26(8):3421–3524, 2022.

[33] Renzo Cavalieri and Andreas Gross. Tropicalization of psi classes. 2024.

[34] J. Rabinoff. Tropical analytic geometry, Newton polygons, and tropical intersections. *Adv. Math.*, 229(6):3192–3255, 2012.